Published in final edited form as:
Agric For Meteorol. 2018 December 15; 263: 308–322. doi:10.1016/j.agrformet.2018.08.028.

Post-disturbance recovery of forest carbon in a temperate forest landscape under climate change

Laura Dobor[a], **Tomáš Hlásny**[a,*], **Werner Rammer**[b], **Ivan Barka**[c], **Jiří Trombik**[a], **Pavol Pavlenda**[c], **Vladimír Šebeň**[c], **Petr Štepánek**[d], **Rupert Seidl**[b]

[a]Czech University of Life Sciences Prague, Faculty of Forestry and Wood Sciences, Kamýcká 129, 165 21 Prague 6, Czech Republic

[b]University of Natural Resources and Life Sciences (BOKU) Vienna, Peter Jordan Straße 82, 1190 Wien, Austria

[c]National Forest Centre – Forest Research Institute Zvolen, T. G. Masaryka 22, 960 92 Zvolen, Slovak Republic

[d]Global Change Research Institute CAS, Belidla 986/4a, Brno 603 00, Czech Republic

Abstract

Disturbances alter composition, structure, and functioning of forest ecosystems, and their legacies persist for decades to centuries. We investigated how temperate forest landscapes may recover their carbon (C) after severe wind and bark beetle disturbance, while being exposed to climate change. We used the forest landscape and disturbance model iLand to quantify (i) the recovery times of the total ecosystem C, (ii) the effect of climate change on C recovery, and (iii) the differential factors contributing to C recovery. We reconstructed a recent disturbance episode (2008–2016) based on Landsat satellite imagery, which affected 39% of the forest area in the 16,000 ha study landscape. We subsequently simulated forest recovery under a continuation of business-asusual management until 2100.

Our results indicated that the recovery of the pre-disturbance C stocks (C payback time) was reached 17 years after the end of the disturbance episode. The C stocks of a theoretical undisturbed development trajectory were reached 30 years after the disturbance episode (C sequestration parity). Drier and warmer climates delayed simulated C recovery. Without the fertilizing effect of CO_2, C payback times were delayed by 5–9 years, while C parity was not reached within the 21st century. Recovery was accelerated by an enhanced C uptake compared to undisturbed conditions (disturbance legacy sink effect) that persisted for 35 years after the disturbance episode.

Future climate could have negative impacts on forest recovery and thus further amplify climate change through C loss from ecosystems, but the effect is strongly contingent on the magnitude and persistence of alleviating CO_2 effects. Our modelling study highlights the need to consider both negative and positive effects of disturbance (i.e., C loss immediately after an event vs. enhanced C uptake of the recovering forest) in order to obtain a comprehensive understanding of disturbance effects on the forest C cycle.

[*]Corresponding author. hlasny@nlcsk.org (T. Hlásny).

Europe PMC Funders Author Manuscripts

Keywords

Disturbance recovery; Norway spruce; Legacy sink; Forest carbon sink; CO_2 fertilization; Central Europe

1 Introduction

Natural disturbances critically affect structure and functioning of forests, and shape spatial patterns in ecosystems (Buma, 2015; Kulakowski et al., 2017; Turner, 2010). Recently, the effect of disturbances on the forest C cycle has been increasingly scrutinized, because forest fires, windstorms and insect outbreaks can cause a release of substantial amounts of carbon (C) from forests to the atmosphere (Liu et al., 2011a; Seidl et al., 2014a), and thus amplify climate change. For example, recent insect outbreaks have turned forests in Canada from a C sink to C source, and future outbreaks have the potential to thwart positive management effects on the forest C balance (Dymond et al., 2010; Kurz et al., 2008a). In Europe, a series of recent large-scale windstorm events, including the storms“Lothar” (1999), “Kyrill (2007)”, “Emma” (2008), “Klaus” (2009) and “Niklas” (2015) (Bonazzi et al., 2012; Fink et al., 2009), severely affected the demography, spatial structure and biogeochemical cycles in forests. These extreme climatic events frequently serve as triggers for biotic disturbance from insect pests, with interactions that have the potential for non-additive outcomes (Buma, 2015; Seidl and Rammer, 2017).

Most forest ecosystems are able to recover from major perturbation within decades to half-centuries (Jones and Schmitz, 2009). However, legacies of forest disturbance events can persist considerably beyond this time frame, and range from altered forest understorey (Bače et al., 2017), to modified stand structure (Seidl et al., 2014a) and the associated susceptibility to subsequent disturbance (Janda et al., 2017). Johnstone et al. (2016) distinguish *information legacies*, such as disturbance adaptation of species, and *material legacies*, such as seed banks, survivors, biomass and nutrient pools. Disturbances typically result in short-term C losses (Lindroth et al., 2009) due to reduced C uptake of the post-disturbance forest (Peters et al., 2013) and increased C losses from respiration (Mayer et al., 2017). This initial post-disturbance C release is subsequently reduced by early-seral species, which swiftly recolonize disturbed areas (Thuille et al., 2000). The resulting C sink of the new tree cohort of recovering forest increases with time since disturbance and culminates at age of ca 10–40 years, depending on forest type (Luyssaert et al., 2007; Zhou et al., 2015). However, increasing drought and excessively large disturbed areas could hamper post-disturbance tree regeneration (Hansen et al., 2018; Harvey et al., 2016), and thus lead to increased C losses after disturbance. For example, Fleischer et al. (2017) reported that a windthrow in the High Tatras Mts. (Slovakia) turned the forest into to a large C source, with the C balance still being negative 10 years after the event. A different pattern of post-disturbance C dynamics was reported by Moore et al. (2013), who found similar declines in gross primary production and respiration, resulting in little change in the net C flux after the severe tree mortality from insects in Colorado, USA.

Disturbances can also induce increased forest growth and C uptake in the decades following the event, resulting in a so-called regrowth sink or legacy sink (Williams et al., 2012; Yue et al., 2016). The mechanisms behind this legacy sink include reduced competition for resources, increased nutrient availability for the tree cohort recovering from disturbance and higher C uptake from young forests and fast-growing early-seral species (e.g. Zhou et al., 2015). Such recovery from natural and human disturbances makes an important contribution to the current terrestrial C sink of the northern hemisphere (e.g., Goodale et al., 2002; Liu et al., 2011a,b; Pan et al., 2011). Yue et al. (2016), for instance, estimated that the current-day forest fire emissions are balanced out by the legacy fire sink in the boreal region.

The future of post-disturbance C recovery remains incompletely understood, causing considerable uncertainty regarding the C cycle effects of natural disturbances in forests (e.g. Metsaranta et al., 2011). The potential effects of climate change further increase the uncertainty of the future role of temperate forests in climate regulation (Thom et al., 2017b). Climate change might intensify forest disturbance regimes in many parts of the world (Seidl et al., 2017a, 2014b), but can have variable effects on the forest C cycle and forest recovery. An elevated atmospheric CO_2 concentration and prolonged vegetation periods resulting from climate change could amplify the C sink effect (e.g., Keenan et al., 2014; Reyer et al., 2014), and contribute to a faster forest recovery after disturbance. However, there is also evidence that even an enhanced net primary production may not be able to offset the C loss from intensified disturbances (Kurz et al., 2008b). Therefore, a better understanding of future forest recovery is essential to improve our understanding of the forest C cycle. Furthermore, recovery is an important indicator of resilience, providing crucial information on the response of ecosystems to changing disturbance regimes (Buma et al., 2013; Seidl et al., 2016).

Here our objectives were to assess how a large-scale stand-replacing disturbance affects the forest C cycle, and to quantify the speed of its recovery. Subsequently, we investigated how future climate change might alter recovery times. We are addressing these questions focusing on a central European mountain forest landscape, which has experienced strong natural disturbances over the last 20 years. Based on theoretical understanding and previous work we hypothesized an initial C loss after disturbance resulting from simultaneously reduced C uptake from NPP (Peters et al., 2013) and increased C release from heterotrophic respiration (Mayer et al., 2017), and a persistent C gain in the decades following the event (as result of vigorous growth of the recovering tree cohort). In particular, we hypothesized the C gain to outweigh the C loss from disturbance after a few decades; i.e. we expected a future legacy C sink from recent disturbances (Williams et al., 2013). Given the mountainous environment of the study region (resulting in plant growth being limited by temperature in the past), we also hypothesized that climate change would have predominately positive effects on tree growth, C uptake and recovery times for our study system.

Empirical investigations of disturbance impacts on forest C and pathways of forest recovery have mainly focused on short-term effects to date (e.g., Lindroth et al., 2009; Mayer et al., 2017). A longer-term perspective on forest C recovery can be gained from applying chronosequence approaches (e.g., Kashian et al., 2013; Zehetgruber et al., 2017). Yet, these

retrospective analyses are not able to account for the potential effects of future changes in the climate system. Therefore we utilized a simulation modelling approach, which allows the consideration of multiple interactive processes affecting the forest C cycle, such as management, disturbances, regeneration of disturbed areas, as well as the consideration of different potential future scenarios of climate.

The quantification of recovery inherently depends on the reference conditions used for defining recovery success. While empirical approaches frequently use the state of the system before a disturbance as such a reference (Lindroth et al., 2009; Lloret et al., 2011; Seidl et al., 2017b), this approach neglects the idiosyncratic nature of any given pre-disturbance system state as well as the natural dynamics of ecosystems. Using simulations allowed us to assess forest recovery against a dynamic reference condition via considering a hypothetical undisturbed development trajectory of our study landscape. Building on C accounting advances from studies of bioenergy systems we specifically calculated (i) the C payback time, when the value of the pre-harvest C is reached, and (ii) the C sequestration parity, when the value of the reference development is reached (Fargione et al., 2008; Lamers et al., 2014; Lamers and Junginger, 2013).

2 Methods and materials

2.1 Simulation model

We used the individual-based forest landscape and disturbance model iLand (Seidl et al., 2012a) to simulate the forest C cycle effects of management, disturbances and climate change. iLand is a process-based ecosystem model that simulates forest landscape dynamics within a hierarchical multi-scale framework (e.g., Mäkelä, 2003), i.e. the model treats different processes at different spatial and temporal scales. The main entity in the model is a tree, for which the demographic processes of growth, mortality, and regeneration are simulated. Processes at the stand and landscape scale constrain the dynamics of individual trees and thus allow for a robust scaling of tree-scale processes to large areas (Seidl et al., 2012a).

Primary production is calculated from the utilizable absorbed photosynthetically active radiation (uAPAR) following a light-use efficiency approach (Landsberg and Waring, 1997). The atmospheric CO_2 concentration modifies production efficiency via a Michaelis-Menten-type equation, and is influenced by environmental factors such as water and nitrogen availability (Friedlingstein et al., 1995). The utilizable fraction of APAR is determined by environmental constraints, which include temperature, vapour pressure deficit, soil water and nutrient availability. Production physiology is calculated at the stand level and the relative contribution of each tree in a stand is determined via its leaf area, absorbed radiation, and species-specific potential to utilize light.

Allocation of assimilated C to tree compartments is based on allometric ratios. The model tracks live C stocks in stem, branch, foliage, coarse root and fine root pools. A closed C cycle is simulated by tracking C in detritus and soil pools. Snags and the transition from snags to downed woody debris (DWD) are simulated explicitly (Thom et al., 2017b). Specifically, tree mortality results in an input of the above-ground C of a tree to the standing

Europe PMC Funders Author Manuscripts

woody debris pool (SWD). C in foliage and fine root compartments of a dead tree are moved to the litter pool in the year of death, while branch and coarse root C are routed to the DWD pool over the five years following death. The remaining SWD C undergoes decomposition, and is eventually transferred to DWD via a species-specific snag half life function. Decomposition rates are dependent on temperature and humidity.

iLand simulates disturbances in a spatially explicit manner and contains process-based modules for a variety of disturbance agents. In addition to disturbances, individual tree mortality is simulated based on species-specific maximum age (Keane et al., 2011) and the occurrence of stress (Seidl et al., 2012a). C starvation is used as a process-oriented indicator of tree stress, and can result from competition for resources as well as suboptimal environmental conditions for tree growth.

Tree regeneration, which is an important process for our analysis of post-disturbance forest recovery, depends on the availability of seeds, which are distributed through the landscape from mature trees via dispersal kernels. Light availability and thermal requirements determine the probability of establishment, provided a seed is present at a 2 × 2 m cell (Seidl et al., 2012b). After establishment, the growth and mortality of saplings up to 4 m in height are simulated in height-based tree cohorts. Traits determining competitive strength are parameterized at the level of tree species (e.g., shade tolerance, drought tolerance, nutrient demand) (Seidl et al., 2012b). These traits together with the dynamically changing environmental conditions (e.g., the shifting light mosaic on the forest floor, the temporal variability in climate conditions) result in the emergence of a dynamic equilibrium of tree species (including the coexistence of species with compatible traits) in the absence of disturbance.

iLand integrates an agent-based model of forest management (Rammer and Seidl, 2015), in which general stand treatment programs are dynamically adapted to the forest state emerging from the simulation. Management interventions are conducted at the level of individual trees, while constraints at the stand-level and management unit-level are observed. We here applied a single forest management agent with consistent management rules across the study landscape (see Section 2.5 for details), but diverse multi-owner landscapes can also be simulated in iLand.

The model was extensively tested and evaluated across a range of ecosystems in Europe and North America in previous studies (Seidl et al., 2012b; Silva Pedro et al., 2015; Thom et al., 2017a). However, this is the first study applying iLand in the Western Carpathians. Therefore, prior to addressing our research questions we extensively evaluated the model performance at our study landscape, following a pattern-oriented approach (Grimm et al., 2005). Specifically, we compared simulated productivity, regeneration and mortality against independent observations (see Section 3.1 below for details).

A comprehensive documentation of iLand as well as model code and executable are available online at http://iLand.boku.ac.at.

2.2 Study region

The study region is located in the Low Tatras Mountains in Slovakia (Lon 20.088–20.275, Lat 48.920–49.061, Central Europe, Western Carpathians) and covers an area of approximately 16,000 ha (Fig. 1a). The forest cover is 70% (*11,200 ha*), and is dominated by Norway spruce (*Picea abies* (L.) Karst.), which makes up 75% of the forest area (8427 *ha*). European larch (*Larix decidua* Mill.) 10% (1154 *ha*), Scots pine (*Pinus sylvestris* L.) 9% (1000 *ha*), Silver fir (*Abies alba* Mill.) 3% (*345 ha*), and European beech (*Fagus sylvatica* L.) 2% (*238 ha*) are other important species on the landscape.

The region is framed by two mountain ridges in the north and south of the landscape, separated by a central valley dominated by non-forest land use. The elevation range is 620–1550 m a.s.l. Air temperature during the growing season (April–September) ranges from 12 to 15 °C, and growing-season precipitation ranges from 380 to 510 mm. Cambisols and Podsols prevail, while Rendzinas occur on calcareous bedrock, which occurs in the highest reaches of the landscape.

The entire forest area is under the stewardship of a private forest management enterprise (ProPopulo). An even-aged management system with a rotation period of approximately 100 years is implemented. The dominant silvicultural approach to tree regeneration in stands with fir and/or beech admixtures is a uniform shelterwood cut. In spruce monocultures, a small-scale clearcutting system is applied. Maximum cutblock size is 3.0 ha in all systems.

Recent years have been characterized by high natural disturbance activity, followed by high levels of salvage and sanitation felling. The natural disturbance regime consists of bark beetles (mainly *Ips typographus* L.) and wind disturbance. In the period 1996–2010, 39% of the forest area was affected by disturbances (Fig. 1b, Supplementary Material 2), as documented by national statistics (Kunca et al., 2015) and remote sensing data. The landscape level growing stock decreased from 4.22 10^6 m^3 in 1996 (average of 380 m^3 ha^{-1}) to 1.93 10^6 m^3 in 2016 (average of 173 m^3 ha^{-1}) (Source: National Forest Centre, Slovakia). At the same time, the landscape-level forest age distribution was substantially shifted towards early-seral stages (Fig. 1c). The landscape and its recent disturbance history is thus typical for many Central European areas that have experienced large-scale disturbances in recent years (Senf et al., 2017).

2.3 Stand and environmental data

Stand and site data were taken from forest management plans (FMP) provided by the National Forest Centre, Slovakia. FMPs contain a polygon vector map that seamlessly covers the entire forest area of the country. Polygons represent forest stands that are described using attributes such as stand structure, species- and cohort-specific mean stand height and diameter, standing volume, site index, mean stand age, stand density, etc. The records are updated via field-based forest inventories in a 10-year cycle.

These data were used to initialize the state of the forest in the landscape simulation model iLand. Specifically, the attributes used were number of trees per hectare, stand age, and diameter at breast height (DBH). Individual tree diameters were randomly drawn from diameter distributions centred on the mean DBH of each stand, with the variance derived

from forest plots in the region. Saplings (trees below 4 m height) were initialized as height cohort with tree height data derived from FMPs.

iLand requires information on soil type and depth and uses plant-available nitrogen (N) as a proxy for nutrient availability. This information was derived on a 100 x 100 m grid from the national forest soil database (National Forest Centre, Slovakia). Because soil depth was only available as categorical variable, depth information for each stand was sampled from a normal distribution centred on the mean soil depth of each of the five depth categories. The variance of the distributions was set to allow a 20% overlap with neighbouring categories to ensure the continuity of the thus derived data. The soil database contained a relative nutrient content (0–1), which was used to estimate the plant-available N (kg ha^{-1} $year^{-1}$) based on iLand-internal model logic (Seidl et al., 2012a).

Daily meteorological data from the nearby meteorological station (Poprad-Ganovce, Slovak Hydrometeorological Institute) was used as a starting point for deriving the climate information necessary for simulation. The landscape was classified into 18 elevation categories, 8 slope categories and 8 aspect categories based on topography, using a grid of 100 × 100 m. Daily minimum and maximum air temperature as well as precipitation data were recalculated to each elevation, slope, and aspect category using the MTClim model (Mountain Microclimate Simulation Model; Hungerford et al., 1989). Eight weather stations in the surrounding of the study region were used to estimate the lapse rate parameters for temperature and precipitation required by MTClim. Daily global radiation data were directly derived from MTClim. Vapour pressure deficit was calculated from downscaled temperature data and observed relative humidity according to Murray (1967).

With regard to possible future climate trajectories, regional climate model (RCM) simulations conducted in the framework of the CORDEX project (Coordinated Regional Climate Downscaling Experiment, Giorgi et al., 2009) were used. Five climate trajectories were generated by the RCM RCA4, driven by the global climate models (GCMs) CM5A-MR, CNRM-CM5, EC-EARTH, MOHC-HADGEM2-ES and MPI-ESM-LR. Two additional climate trajectories were generated by the RCMs HIRHAM5 and RACMO22E, which were both driven by the GCM EC-EARTH (see Appendix A for more details on the climate models used). Each GCM-RCM combination was driven by two Representative Concentration Pathway (RCP) scenarios (RCP4.5 and RCP8.5; Moss et al., 2010), resulting in 14 projections of future climate considered in the analysis. Weather station data were used for bias correction of the RCM outputs using the procedure described in Štepánek et al. (2016). Data for all climate scenarios were recalculated to a 100 m grid within the study region using a single RCM grid cell located within the landscape, and applying the same method as used for observational data (Table 1.). CO_2 concentrations used to drive the forest simulations were defined by the two RCP scenarios used, and reached 538 ppm and 936 ppm in 2100 under RCP4.5 and RCP8.5 runs, respectively.

2.4 Model evaluation

Productivity testing was based on a comparison of measured and simulated site indices (SI), defined as the stand height at age 100 years. Simulations of monospecific stands with an initial age of 30 years were run based on the stem number trajectories defined in national

Europe PMC Funders Author Manuscripts

yield tables for the respective SIs (Halaj and Petráš, 1998). Productivity tests focused on the five most abundant species in the region – Norway spruce, European beech, European larch, Scots pine and Silver fir. Two testing datasets were used – FMP data and National Forest Inventory data (Source: National Forest Centre, Slovakia). For the FMP-based testing, 80–130 forest stands in which the focal species occurred were selected randomly throughout the landscape. For the NFI-based testing, 31 plots distributed in a regular 4 × 4 km grid in and around the study region were used (see Supplementary Material 1 for more details).

Given the limited availability of empirical mortality data, we tested the reliability of the simulated mortality against the self-thinning coefficients of Reineke (1933) and Yoda et al. (1963). Mortality testing used the same simulation design as the productivity evaluation, but without simulating tree removal through management.

Long-term forest dynamics was tested by comparing the species composition emerging from the simulations after 2000 simulation years without disturbance to the natural vegetation map of the region (Rizman et al., 2005). These simulations were started from bare ground, were run using reference climate (i.e. a climate series generated by random sampling of years from the period 1970–2000 with replacement), and assumed background levels of seed input from all species across the landscape. In addition to the evaluation of the tree species composition emerging at the end of the simulation period also the ecological plausibility of species succession over the course of the simulation was assessed.

2.5 Study design and recovery indicators

Prior to scenario simulations a 600-year spin-up run was performed to estimate the initial litter, dead wood and soil C pools. The spin-up was also used to determine the spatial position of individual trees within a stand, information that cannot be extracted from the available inventory data. The spin-up duration was chosen based on the natural disturbance rotation period in the region, corresponding to twice the average rotation period calculated for managed forests (Thom et al., 2013) and extending to the rotation period derived for the most severe natural disturbance events recorded in primeval forests (Janda et al., 2017). The spin-up started from bare ground with seeds of all species being available. For each stand, the stand structure as recorded in the FMP from 1996 (initial year of simulation) was set as target value. Management was considered during the spin-up period. After 400 spin-up years had elapsed the spin-up was stopped individually for each stand when the simulated stand structure matched the FMP target values. The initial year of our analysis was 1996, and both stand structure and pool sizes for the soil, litter and dead wood C pools were derived by means of the above described spin-up procedure.

For each year in the period 1996–2016 we imposed the observed pattern of disturbances in the simulation, with the main disturbance event occurring in the period 2008-2016. Disturbance extent and location were taken from Landsat data (see Fig. 1 and Supplementary Material 2), while disturbance severity was deduced from FMP data. The share of timber disturbed by wind and bark beetles was set to 50:50 for all years except for the year 2008, when a major windstorm affected the landscape and 80% of disturbance was assumed to be due to wind.

Management of the landscape was simulated dynamically, i.e. with operations adapted to the stand conditions emerging in the simulation (based on Rammer and Seidl, 2015). The applied forest management strategy was simulated based on the same set of rules in all simulation runs and remained the same over the entire study period 1996–2100. Management measures included tending, thinning and harvesting, with timing and intensity of operations modelled after the management practice currently applied in the region (Halaj and Petráš, 1998). Depending on the SI, 3–4 thinning operations were applied and rotation periods ranged from 90 to 140 years. In spruce monocultures a clearcut system was applied, while a shelterwood system was simulated in mixed stands. Management also included salvaging of disturbed timber, with an extraction rate of 60%. Following the practice currently applied in the region, tree stems were removed by salvaging, while branches and roots remained in the forest.

To obtain a dynamic baseline for assessing disturbance recovery we ran an additional simulation applying the same study design as described above, but without imposing disturbances in the period 1996–2016. In all runs no further disturbances were simulated beyond 2016, in order to study the recovery from the recent disturbance episode and control for compounding effects of subsequent disturbances.

To evaluate the effect of climate change on disturbance recovery, we ran simulations under reference climate and the 14 climate change scenarios. For simulations under reference climate we created a climate time series for 1996–2100 by randomly sampling years with replacement from the period 1971–2000, and keeping the CO_2 concentration constant at 367 ppm. The entire simulation experiment thus consisted of 31 simulation runs: spin-up + (disturbed + undisturbed) × (reference climate + RCP4.5 × 7 RCMs + RCP8.5 × 7 RCMs).

To investigate the recovery of total forest C (C_{total}) after the disturbance episode of 2008–2016, we adopted methodological advances in C accounting emerging from the evaluation of bioenergy systems (Fargione et al., 2008). Contrary to the original use of the concept, we here focus only on C in the ecosystem, and do not consider effects related to C in wood products, bioenergy, fossil fuel substitution or supply chain emissions. Specifically, two indicators were calculated, C parity and C payback time. C parity describes the time needed to reach the C level of the hypothetical undisturbed development of the landscape (Fig. 2)(Fargione et al., 2008; Lamers et al., 2014; Lamers and Junginger, 2013). It is calculated as:

$$Parity = \sum_{i=1}^{n} \begin{cases} 1, & if\ DistCtotal_i < \mathrm{Ref}Ctotal_i \\ 0, & if\ DistCtotal_i > \mathrm{Ref}Ctotal_i \end{cases}$$

$RefCtotal_i$ is the total ecosystem C of an undisturbed reference simulation in year i. i is counted from the last year of the disturbance episode (2016), n is the number of simulation years from the end of disturbance episode. The second indicator, C payback time (also referred to repayment time or C break-even), quantifies the number of years needed to reach the pre-disturbance C level (Fig. 2), i.e.:

$$Payback = \sum_{i=1}^{n} \begin{Bmatrix} 1, \ if \ DistCtotal_i < Ctotal_{predist} \\ 0, \ if \ DistCtotal_i > Ctotal_{predist} \end{Bmatrix}$$

$DistCtotal_i$ is the total ecosystem C of the disturbed simulation in year i, $Ctotal_{predist}$ is the total ecosystem C prior to disturbance (2007 in the current study). As the disturbed and reference run diverged slightly already in 2007, we averaged over both trajectories for determining $Ctotal_{predist}$ (Fig. 2).

To investigate the effects of future climate on C cycle recovery in greater detail, we explored the response of payback and parity times to the projected changes in selected climate variables across the 14 studied climate trajectories (7 RCMs × 2 RCPs). Specifically, we evaluated trends in payback and parity times across the between-scenario climate variation in the period 2030–2060 (including reference climate), i.e. the time period during which most of the simulations reached C payback and parity.

To better understand the drivers of simulated forest recovery, we isolated the effects of changes in climate variables from changes in atmospheric CO_2 concentration. To that end, an additional set of simulations were run under changing climate, while keeping the CO_2 concentration constant at the reference level of 367 ppm. To quantify the effect of climate alone, we contrasted simulations driven by reference climate with simulations under climate change, with both sets run under reference CO_2 conditions. To isolate the effect of CO_2, we compared simulations driven by changing climate and projected future CO_2 concentrations to simulations under a changing climate and reference CO_2 levels.

Finally, we analysed the mechanisms driving C recovery by individually investigating the main components of the forest C cycle during and after disturbance. Specifically, the investigated fluxes were: Gross Primary Productivity (GPP); Net Ecosystem Production (NEP = GPP - Reco), where Reco = (R_{auto} + R_h), with R_{auto} denoting autotrophic respiration and R_h heterotrophic respiration; and Net Ecosystem Carbon Balance (NECB = NEP + management C loss) (Chapin et al., 2006). C in living biomass (C_{living}), which includes aboveground compartments and roots, was used as an indicator of lateral C fluxes related to harvests and salvaging. All analyses of simulation results were conducted using R v.3.3.2 (R Core Team, 2016).

3 Results

3.1 Model evaluation

Productivity differences throughout the landscape were generally well captured by iLand, based on the comparison of simulated and observed SI, with an overall proportion of the variance explained of 0.67 when tested against FMP data. However, model performance differed between tree species and reference datasets (FMP and NFI) (Table 2). Productivity of the dominating Norway spruce was simulated with moderate accuracy compared to FMP data (R^2 0.52), but showed only poor correspondence to NFI data (R^2 0.16). European beech and silver fir consistently performed well against both reference datasets (R^2 0.70 – 0.94). European larch also performed well (R^2 0.87), while Scots pine simulations showed the

Europe PMC Funders Author Manuscripts

overall lowest correspondence to reference data (R^2 0.01 – 0.31). Simulated SI had a minor but not significant bias when compared to FMP-based SI across all species, while the bias was significant when NFI-based SI values were used as reference. Simulated SI values also tended to have lower overall variability compared to reference data.

The comparison of simulated tree mortality against the self-thinning coefficients of Reineke (-1.605) and Yoda (-0.5) showed the expected reduction in stem number with increasing tree size and stand biomass. Although there were differences in the coefficients between species, the average coefficient across all-species was −1.73 ± 0.21 for Reineke and −0.53 ± 0.17 for Yoda, corresponding well to the theoretical expectations (see Supplementary Material 1 for details).

In the simulation of undisturbed long-term forest development, Norway spruce, European beech and silver fir dominated the tree species composition after approximately 300 simulation years (Supplementary Material 1). The emerging dominance of these species is in good correspondence with the expected potential natural vegetation of the region. A large share of pioneer species (e.g., *Betula pendula, Alnus nigra*) and light demanding species (L. *decidua*) in the early stage of the simulation underline the models' ability to simulate realistic trajectories of forest succession from early to late-seral species.

3.2 Recovery of total ecosystem carbon

3.2.1 Carbon payback time and sequestration parity—The model simulated a substantial decrease in C_{total} from regular harvests in the pre-disturbance period and from salvaging during the disturbance episode (Fig. 3). Under reference climate, the total removed C in the period 1996–2016 was 35 t ha^{-1} (regular harvest) and 53 t ha^{-1} (salvage cutting). The minimum level of C_{total} (339 t ha^{-1}) was reached in 2017. During the disturbance episode (2008–2016), C_{total} decreased by 15% relative to the reference year 2007 (399 t ha^{-1}), representing an average landscape-level C loss of 61 t ha^{-1}.

Under reference climate, C payback was reached after 17 years (in 2033), when the C_{total} of the disturbed simulations exceeded the pre-disturbance value (2007). In 2046 also C parity was reached, i.e. the C_{total} of the disturbed simulations reached the level of the simulations without disturbance after 30 years. Climate change modified the simulated trajectories of C_{total} mainly in the second half of the century. Therefore, the multi-model means of payback and parity did not show any significant departure from values obtained under reference climate.

Disregarding the CO_2 fertilization effect by keeping CO_2 levels constant at the reference level delayed C payback times by 2 and 4 years under RCP4.5 and RCP8.5 scenarios, respectively (PB2, Fig. 3). With the exception of one run under RCP8.5, all simulations reached C payback within the 21st century also without CO_2 fertilization. In contrast, C parity was generally not obtained until 2100 under RCP8.5 if the atmospheric CO_2 level was kept constant at the reference level. This indicates that a strong CO_2 fertilization effect is a crucial driver of the simulated future C recovery.

3.2.2 The effects of climate and CO_2 fertilization on carbon recovery—

Given the prominent role of CO_2 fertilization in the simulated recovery of C_{total} (Fig. 3), we further investigated the effects of changing climate and elevated CO_2. Elevated CO_2 concentration caused C_{total} to increase under both RCPs. The increase was more pronounced under RCP8.5 than under RCP4.5, with differences being roughly proportional to difference in CO_2 concentrations (Fig. 4). The isolated effect of climate (i.e. without the effect of CO_2 fertilization) caused a substantial decrease in C_{total}. The combined effect of changing climate and elevated CO_2 caused C_{total} to oscillate around the reference development until 2060, with a distinct period of negative values between 2000 and 2020. After 2060 the positive effect of elevated CO_2 compensated the negative effects of changing climate and C_{total} started to increase. The increase persisted until the end of simulation period. Complementary information on the response of C fluxes to elevated CO_2 can be found in Supplementary Material 3.

To more explicitly investigate the effect of climate change we analysed C recovery over the climate signal contained in the studied climate scenarios. The change in growing season air temperature and growing season precipitation represented by the 14 climate scenarios studied ranged between 1.2–3.0 °C and -60 – 60 mm, respectively (period 2031–2060 relative to reference climate 1971–2000; see Table 1 and Appendix A). The amount of years needed to reach recovery consistently increased with decreasing precipitation. For C parity, the increase was +3.6 years in response to a 10% reduction in precipitation ($p = 0.13$; Fig. 5). A similar response to precipitation change was found for C payback time ($p = 0.22$). A warmer climate also extended the payback time by ca. 1 year in response to a 1 °C temperature increase ($p = 0.21$). We thus find indications that C recovery was slowed under drier and warmer climatic conditions.

3.3 Carbon dynamics

3.3.1 Immediate disturbance impact—

The disturbance affected 39% of the forest area in the landscape, causing a reduction in forest leaf area by 27% during 2008. As a consequence, GPP was strongly reduced (Appendix C) for a period of roughly 6 years after the event, with R_a following a similar pattern (Fig. 6).

Simulated C stored in live tree C compartments (stems, branches, foliage, coarse and fine roots) strongly decreased as a result of the main disturbance impact in 2008 (Appendix B). In 2008, also a large portion of C was removed by salvage cutting, while C removal by regular harvests ceased due to the disturbance (Fig. 3). At the same time, dead trees that were not salvaged and C in compartments not affected by salvage operations (i.e., 40% of stem C, and 100% of branch and foliage C of the trees killed in the disturbance episode) created a substantial influx into the litter, downed and standing woody debris pools on the landscape (Appendix B).

Decomposition caused a short-term increase in R_h, which exceeded the level of undisturbed development by up to 2.3 tC ha^{-1} $year^{-1}$. The difference between disturbed and undisturbed R_h was highest in the year following the main disturbance impact (2009), what was related mainly to fast decomposition of leaves and branches. Slower decomposition of larger

diameter woody residues caused R_h to remain elevated until 2016. In subsequent years R_h oscillated around the level of the undisturbed forest.

Together, the developments of GPP and respiration reduced NEP significantly during the disturbance episode, and the landscape turned to a net C source for seven years. In these years the total amount of C release was 118 10^3 tC, which corresponds to 3.5 years of C uptake of the undisturbed landscape. The cumulative difference between the undisturbed and disturbed NEP trajectories during 2008–2018 was 53 tC ha^{-1} (592 10^3 tC at the landscape level; Fig. 7; red and pink polygons), corresponding to approximately 17 years of undisturbed C uptake. In terms of NECB, the maximum net C loss was an order of magnitude larger than NEP (ca -2 vs. -15 tC ha^{-1} $year^{-1}$). The cumulative difference between undisturbed and disturbed NECB was 83 tC ha^{-1} (935 tC on landscape level) for the 10-year period 2008–2018.

3.3.2 Long-term disturbance impact—Development in the post-disturbance period was characterized by substantially elevated GPP relative to undisturbed development, which persisted for 35 years (2019–2055) under reference climate. At the same time, R_h did not significantly differ from the undisturbed development. Consequently, the differential developments of GPP and respiration generated a legacy sink effect after 2018, which contributed significantly to the recovery of C_{total} from the disturbance event. Under reference climate, the cumulative C gain from this legacy sink was 55 tC ha^{-1} for NEP and 98 tC ha^{-1} for NECB (617 10^3 tC and 1010 10^3 tC at the landscape scale, respectively) (Fig. 7; green polygons).

Climate change amplified GPP already in the first decades after the disturbance episode, the effect was, however, most pronounced after 2050. The main drivers of GPP increase were elevated air temperature and CO_2 concentration (Supplementary Material 3). At the same time, climate change also increased R_h in the post-disturbance period (Fig. 6) relative to reference climate. The mean difference during period 2050–2100 was +1.6 tC $year^{-1}$ and +2.6 tC $year^{-1}$ under RCP4.5 and RCP8.5, respectively. The increase was mainly driven by increased input due to elevated GPP, but also higher temperatures contributed to an increased level of R_h (Supplementary Material 3).

Together these processes led to an amplified legacy sink effect under climate change. In particular, the amount of C accumulated in the period with legacy sink (Fig. 7; green polygons) increased by 5 and 7 tC ha^{-1} under RCP4.5 and RCP8.5 scenarios, respectively. In contrast, climate change had no significant effect on the legacy sink effect in terms on NECB.

Overall, the coupled effect of disturbance and climate change on NEP and NECB persisted until 2050; 34 years after the end of disturbance episode no difference between disturbed and undisturbed simulations could be detected (Fig. 7). However, the underlying fluxes (GPP, R_a and R_h) showed significant departure from the undisturbed development also in the second half of the 21st century (Fig. 5).

4 Discussion

Previous research has indicated that disturbances can alter trajectories of forest C in diverse ways (Bradford et al., 2012; Liu et al., 2011b) and that it might take decades to recover disturbance-related C losses. Consistent with empirical research, our simulation study showed that a severe disturbance might turn a forest landscape into a net C source, and that it takes several decades to compensate the C loss from disturbance. We identified CO_2 fertilization as a prominent driver facilitating recovery in a temperate forest landscape. Drier and warmer climate, on the other hand, could slow down the recovery processes under climate change. We also corroborated the presence of an enhanced C sink following disturbance. This legacy sink effect has not yet been sufficiently recognized in considerations of the C impact of disturbances in Europe's forests (Seidl et al., 2014b). Our finding that such a legacy sink effect can persist for decades (Foster et al., 1998) highlights the importance of considering post-disturbance forest development in deliberations of the climate regulation function of forests.

4.1 Model evaluation

Process-based ecosystem models are required to assess the potential impacts of events such as disturbances in a no-analogue future (Gustafson, 2013). Such models are usually not calibrated with local data but are based on first principles of ecology. Consequently, testing these models against local data is important to ensure that the eco-system dynamics of the studied system is adequately captured in the model (González-García et al., 2016; Minunno et al., 2010; Seidl et al., 2012b). To that end we here performed a number of model evaluation exercises prior to model application, following the pattern-oriented modelling approach suggested by Grimm et al. (2005).

Productivity tests showed substantial differences between tree species, and also between the two reference datasets used for testing. Simulated SI matched observations better for FMP data compared to NFI data. A reason for this deviation could be the different spatial grain of the two reference data sets: NFI data represent single inventory plots, and thus contain the full variability regarding micro-site conditions and individual tree development. FMP data, on the other hand, represent stand level estimates, derived by averaging several sample plots taken within each stand (i.e., three plots with an area of 0.045 ha per ha of forest stand for the FMP data used here). Stand-level differences within the landscape are thus better captured by FMP data, while NFI data are better at describing the large-scale variation within the ecosystem. As the driver data used to run the model mainly represented differences at the stand level while largely neglecting fine-scale environmental heterogeneity (e.g. soil data were derived from several soil samples, and subsequently averaged over a forest stand), a better correspondence of model simulations with FMP data is consistent with expectations. More broadly, our finding highlights the importance of considering appropriate datasets for model testing, a field that warrants further research (e.g., Mina et al., 2016; van Oijen et al., 2013; Zhu and Zhuang, 2013).

Overall, iLand was well able to represent typical forest dynamics in the forests of the Western Carpathians. The achieved correspondence between observed and simulated productivity (species-averaged R-squared of 0.67 relative to FMP data, and considerably

higher values for important species such as beech with an R-squared 0.89, and fir with 0.74) was well within the range of previous model applications. For example, Seidl et al. (2012a) reported a species-averaged R-squared between observed and simulated SI of 0.63 for the Cascade Mts. (Oregon, USA) and 0.83 for the Eastern Alps (Austria). Similar results for the Eastern Alps were reported by Thom et al. (2017a). This satisfactorily performance of the model in the current study region is important as the present study is the first application of the model in the Carpathian Mountains. Based on the tests conducted here we conclude that iLand is generally applicable to study forest dynamics also in Central-Eastern European forest ecosystems. A good correspondence of the simulated C balance with theoretical expectations and results of empirical studies also supports this conclusion.

4.2 Post-disturbance recovery of forest carbon

We showed that the effect of a single high-severity disturbance event on the forest C can persist several decades. Our simulated multi-decadal recovery times are in agreement with previous modelling studies (Wang et al., 2014; Yue et al., 2016) as well as with empirical research (Bače et al., 2017; Janda et al., 2017) from different forest types and environmental conditions. While recovery of the pre-disturbance C (payback time) was reached 17 years after the end of disturbance episode, C parity was achieved only after 30 years. Similarly, Aguilos et al. (2014) reported that mixed forest replaced by a larch plantation required 8 to 34 years to fully recover the CO_2 that was emitted after the clearing. In contrast, a review by Fu et al. (2017) indicated that forest recovery times largely varied between disturbance types and C cycle indicators considered, with the longest recovery times of total biomass (104 ± 33 years) and the shortest of C fluxes (23 ± 5 years). Our recovery time estimates for C_{total} were substantially shorter, which can be explained by the fact that only 39% of the forest area was disturbed, and the disturbed sites were rapidly replanted with fast-growing Norway spruce in our study area.

Simulations under climate change showed diverging effects of climatic drivers and atmospheric CO_2 on the recovery of the forest C, particularly for C parity. While climate change delayed the achievement of C parity, increasing CO_2 concentration compensated this delay. In contrast, simulations disregarding CO_2 fertilization effect resulted in parity times that exceeded our simulation period. This finding of a prominent role of atmospheric CO_2 in forest C uptake is in agreement with the works of Solberg et al. (2009) and Bellassen and Luyssaert (2014), who suggest that elevated atmospheric CO_2 concentrations is – in addition to increased nitrogen deposition – the main driver of the current global forest C sink. Also Yue et al. (2016) reported an amelioration of the forest fire legacy C sink by climate warming and CO_2 fertilization for the boreal biome. However, limited experimental knowledge of the long-term responses of plants to CO_2 enrichment makes simulation studies heavily dependent on assumptions regarding the persistence of CO_2 fertilization (Buckley, 2008; Reyer et al., 2014). Here we used a Michaelis-Menten formulation to approximate CO_2 response (Friedlingstein et al., 1995), which considers the effect of atmospheric CO_2 on productivity, and accounts for amplified effects under water limitation and downregulation when nitrogen is limiting. However, we assumed the base CO_2 response $\beta 0$ to be constant over time, neglecting potential adaptations of tree ontogeny or leaf physiology. Such an approach is tentatively supported by the analysis of Friedlingstein et al. (1999), finding very

little allocation changes in response to CO_2 changes in temperate forests. On the other hand, some empirical studies suggest that acclimation of photosynthetic and respiratory processes to elevated CO_2 might be important, mainly when long-term effects are considered (Buckley, 2008; Hanson et al., 2005; Medlyn et al., 2001; Smith and Dukes, 2012). In summary, the strong response of C recovery to elevated CO_2 and the remaining uncertainties regarding this process (Hyvönen et al., 2007; Lindner et al., 2014) warrant further research.

We found longer recovery times of C_{total} under drier and warmer conditions. The fact that our results in this regard were not statistically significant should not detract from the general signal in the data, as statistical significance is not a strong means of inference in simulated data (see e.g. White et al., 2014). Furthermore, we here studied the recovery from a recent disturbance event, for which the climate signal was only moderate, ranging from +1° to + 3 °C and from -60 to + 60 mm. However, disturbances are expected to increase throughout the 21st century in Central Europe (Thom et al., 2017b), and the climatic conditions for recovery from a similar event as the one investigated here would be drastically different in the future. For the end of the 21st century, ten out of the 14 climate projections used here indicates a decrease in precipitation (Appendix A), which could substantially hamper the capacity of forests to recover from disturbances (Hansen et al., 2018). This is in line with studies that indicate a possible global reduction in the efficiency of the terrestrial C sink due to drought (Anderegg et al., 2015; Zeng et al., 2005; Zhao and Running, 2010).

4.3 Forest C dynamics

The simulated trajectory of NEP under disturbance agreed well with theoretical expectation (e.g. Chapin et al., 2006, 2002; Goulden et al., 2010), suggesting that forest ecosystems become a C source immediately after stand-replacing disturbances due to reduced C uptake of the post-disturbance forest (Peters et al., 2013) and increased C losses from respiration (Mayer et al., 2017). The study landscape was a C source for seven years with NEP and eleven years with NECB under reference climate. This is in line with, for example, values reported by Wang et al. (2014) (negative NEP for 6–17 years and stabilized C sink after 60 years) for the deciduous broadleaved and evergreen coniferous forests in Michigan and Wisconsin (USA). Similarly, Amiro et al. (2010) reported that the C sink of disturbed forest ecosystems in North America had recovered 10 years after a disturbance. Goulden et al. (2010) found that the transition of the post-fire boreal forest from a C source to a C sink occurred within 11–12 years. Our results fall well within the range of values reported in the literature, suggesting the utility of our simulation approach for quantifying C parity and payback time.

The simulated decrease in NEP in our study could be attributed to substantially decreased GPP and relatively minor increases in R_h, which is in agreement with the findings of, for example, Lindroth et al. (2009) and Peters et al. (2013). Similarly, Goulden et al. (2010) suggest that the loss of detritus proceeds more rapidly than the new accumulation of live biomass after disturbance, resulting in an initial loss of total carbon (i.e. negative NEP). However, multiple switches between periods of C uptake and release after a disturbance, as recently reported by Amiro et al. (2006) and Goulden et al. (2010), could not be observed in our results.

Our finding of a legacy sink effect is consistent with empirical studies from diverse environments (e.g. Williams et al., 2013; Yue et al., 2016), and is one of the first reports for such an effect for temperate forest landscapes. From the perspective of C dynamics, the effect emerged from C gains from increased GPP outweighing C losses from respiration. From the perspective of vegetation dynamics the increased GPP leading to the legacy sink emerged from several interacting processes, among which the vigorous regrowth of a young cohort of trees (around the age of optimal growth performance) was the most prominent one (Chapin et al., 2002; Goulden et al., 2010). However, a change in species composition after disturbance (i.e. towards early-seral species) did not simultaneously occur, because extensive planting of lateseral target tree species controlled natural successional dynamics in our study system (Appendix C). Increased nutrient input from decomposing post-disturbance residues is another mechanism that can result in a legacy sink effect (Fernández-Martínez et al., 2014), but was not explicitly considered here.

4.4 Methodological considerations

We adopted an approach for quantifying C recovery that considers both static and dynamic reference values. Such approaches have been previously used mainly in estimating the impacts of bioenergy systems, including changes in land-use, C storage in wood products, or fossil fuel displacement effect (Fargione et al., 2008; Gibbs et al., 2008; Lamers and Junginger, 2013). We here followed this approach for an assessment of forest ecosystem C, and highlighted its utility also for assessing disturbance impact in forest landscapes. Assessments of C recovery after disturbance fundamentally depend on the reference condition for recovery that is being used. This is underlined by our finding of considerable differences in recovery times between static (C payback time) and dynamic (C parity) baselines, which were 17 and 32 years respectively. Differences of similar magnitude were reported also in other studies, although differences in the representation of vegetation and the definition of a dynamic reference condition decisively affect outcomes (Lamers and Junginger, 2013). Considering the pre-disturbance C as reference condition is a frequently used approach in the assessment of recovery and resilience (Aguilos et al., 2014; Lindroth et al., 2009; Lloret et al., 2011; Seidl et al., 2017b), and is also used in the assessment of the impacts of changes in land use and land management (e.g. Gibbs et al., 2008). There are clear advantages to this approach, as a pre-disturbance state can often be derived from observational data, and a comparison between pre- and post-disturbance states can be easily communicated. Such an approach might be, however, too simplistic, as it neglects the dynamic changes in the ecosystem that would have occurred in the absence of disturbance. Specifically, a static baseline neglects the additional C uptake of an undisturbed forest, leading to an underestimation of disturbance impacts and recovery times. Dynamic baselines are thus recommended. They do, however, require the careful definition of business-as-usual management for the derivation of dynamic reference conditions (Lamers and Junginger, 2013). Such dynamic baselines can be obtained from simulation models, as was demonstrated here using the model iLand. Similarly, Lamers et al. (2014) used the Carbon Budget Model of the Canadian Forest Sector, and Jonker et al. (2014) used the model GORCAM. In empirical studies the approach to consider a dynamic reference is via undisturbed control plots or a BACI (before-after-control-impact) study design (Conner et al., 2016).

Europe PMC Funders Author Manuscripts

Some factors potentially affecting post-disturbance recovery were not considered in the current study. Adapted management measures can, for instance, substantially modify recovery times via planting and tree species selection. We, however, considered a continuation of the currently applied management in the region under all simulated scenarios. Selecting tree species with different climate sensitivity might also significantly alter patterns of C uptake in the 21st century post disturbance. Efforts to convert drought-prone spruce forests have intensified in Europe in recent decades (Hlásny et al., 2017; Spiecker et al., 2004), and promoting tree species such as European beech and Douglas-fir (*Pseudotsuga menziesii*) (Albrecht et al., 2013; Thomas et al., 2015) might reduce the climate sensitivity of the forest C cycle (Seidl et al., 2018; Thom et al., 2017b). Also, alterations of salvaging intensity can have strong effects on total ecosystem C and the rate of heterotrophic respiration (Bradford et al., 2012). However, salvaging might also mitigate bark beetle outbreaks (Stadelmann et al., 2013), and thus affect the overall forest C balance positively. The net effect of salvage logging on forest C thus remains unclear.

Finally, it is important to note that we assumed disturbance-free forest development after the focal disturbance period studied here. This allowed us to isolate the recovery from the focal disturbance episode from other transient changes in the ecosystem. However, our analysis consequently neglects compounding effect of potential subsequent disturbances. The fact that interactions between disturbances have the potential to result in non-additive outcomes (Buma, 2015; Seidl and Rammer, 2017) suggests that additional disturbances could substantially alter recovery trajectories. Given that disturbance return intervals in Central European forests are usually greater than 100 years (Janda et al., 2017; Thom et al., 2013), our approach to neglect the effect of subsequent disturbances is a reasonable first approximation. The plausibility of the presented recovery times and their agreement with empirical studies further underlines the utility of our approach. However, if disturbances substantially increase in the future, as expected by a number of studies (Seidl et al., 2017a, 2014b), it will become increasing important to study the effects of compound disturbances on forest recovery (Buma, 2015; Johnstone et al., 2016; Seidl and Rammer, 2017).

5 Conclusions

We here focus on a managed Norway spruce forest ecosystem, which is a widely distributed forest type in the temperate biome of Europe. Despite the ecological and societal importance of these forests, research to date has largely focused on productivity, while other processes, such as recovery after disturbance, remain understudied. Our simulation study contributes to an improved understanding of disturbance effects on C cycling in these forests, and highlights that high severity disturbances constitute an extensive perturbation of their C cycle. Moreover, we identified and quantified a legacy sink effect after disturbance in our study system. This suggests that both positive and negative C cycle impacts of disturbances have to be considered in order to comprehensively assess their effect on the climate regulating function of forests. The climate sensitivity of the identified legacy sink as well as the prominent role of CO_2 fertilization in recovery highlight the importance of applying process-based simulation approaches for estimating the future of the forest C cycle.

Supplementary Material

Refer to Web version on PubMed Central for supplementary material.

Acknowledgements

This study was supported by the grants "EVA4.0", No. CZ.02.1.01/0.0/0.0/16_019/0000803 and "EXTEMIT - K", No. CZ.02.1.01/0.0/0.0/15_003/0000433 financed by OP RDE; Austrian Science Fund FWF START grant no. Y895-B25; projects of the Ministry of Education, Science, Research and Sport of the Slovak Republic under contracts no. APVV-15-04-13 and APVV-16-03-25; and EC COST Action FP1304 (PROFOUND).

References

Aguilos M, Takagi K, Liang N, Ueyama M, Fukuzawa K, Nomura M, Kishida O, Fukazawa T, Takahashi H, Kotsuka C, Sakai R, et al. Dynamics of ecosystem carbon balance recovering from a clear-cutting in a cool-temperate forest. Agric For Meteorol. 2014; 197: 26–39. DOI: 10.1016/j.agrformet.2014.06.002

Albrecht AT, Kohnle U, Hanewinkel M, Bauhus J. Storm damage of Douglas-fir unexpectedly high compared to Norway spruce. Ann For Sci. 2013; 70: 195–207. DOI: 10.1007/s13595-012-0244-x

Amiro BD, Orchansky AL, Barr AG, Black TA, Chambers SD, Chapin FS, Goulden ML, Litvak M, Liu HP, McCaughey JH, McMillan A, et al. The effect of post-fire stand age on the boreal forest energy balance. Agric For Meteorol. 2006; 140: 41–50. DOI: 10.1016/j.agrformet.2006.02.014

Amiro BD, Barr AG, Barr JG, Black TA, Bracho R, Brown M, Chen J, Clark KL, Davis KJ, Desai AR, Dore S, et al. Ecosystem carbon dioxide fluxes after disturbance in forests of North America. J Geophys Res. 2010; 115 G00K02 doi: 10.1029/2010JG001390

Anderegg WRL, Schwalm C, Biondi F, Camarero JJ, Koch G, Litvak M, Ogle K, Shaw JD, Shevliakova E, Williams AP, Wolf A, et al. Pervasive drought legacies in forest ecosystems and their implications for carbon cycle models. Science (80-.). 2015; 349: 528–532. DOI: 10.1126/science.aab1833

Bače R, Schurman JS, Brabec M, Cada V, Després T, Janda P, Lábusová J, Mikoláš M, Morrissey RC, Mrhalová H, Nagel TA, et al. Long-term responses of canopy–understorey interactions to disturbance severity in primary Picea abies forests. J Veg Sci. 2017; 28: 1128–1139. DOI: 10.1111/jvs.12581

Bellassen V, Luyssaert S. Carbon sequestration: managing forests in uncertain times. Nature. 2014; 506: 153–155. DOI: 10.1038/506153a [PubMed: 24527499]

Bonazzi A, Cusack S, Mitas C, Jewson S. Spatial structure of European storms model validation based on the univariate distribution of wind speeds. Nat Hazards Earth Syst Sci Discuss. 2012; 12: 1769–1782. DOI: 10.5194/nhess-12-1769-2012

Bradford JB, Fraver S, Milo AM, D'Amato AW, Palik B, Shinneman DJ. Effects of multiple interacting disturbances and salvage logging on forest carbon stocks. For Ecol Manag. 2012; 267: 209–214. DOI: 10.1016/j.foreco.2011.12.010

Buckley TN. The role of stomatal acclimation in modelling tree adaptation to high CO2. J Exp Bot. 2008; 59: 1951–1961. DOI: 10.1093/jxb/erm234 [PubMed: 18000018]

Buma B. Disturbance interactions: characterization, prediction, and the potential for cascading effects. Ecosphere. 2015; 6: 1–15. DOI: 10.1890/ES15-00058.1

Buma B, Brown CD, Donato DC, Fontaine JB, Johnstone JF. The impacts of changing disturbance regimes on serotinous plant populations and communities. Bioscience. 2013; 63: 866–876. DOI: 10.1525/bio.2013.63.11.5

Chapin, FS, Matson, PA, Mooney, HA. Principles of Terrestrial Ecosystem Ecology. Springer-Verlag; New York: 2002.

Chapin FS, Woodwell GM, Randerson JT, Rastetter EB, Lovett GM, Baldocchi DD, Clark DA, Harmon ME, Schimel DS, Valentini R, Wirth C, et al. Reconciling carbon-cycle concepts, terminology, and methods. Ecosystems. 2006; 9: 1041–1050. DOI: 10.1007/s10021-005-0105-7

Christensen, OB, Drews, M, Christensen, JH, Dethloff, K, Ketelsen, K, Hebestadt, I, Rinke, A. The HIRHAM Regional Climate Model Version 5 (β), DMI Techical Report. Copenhagen: 2007.

Conner MM, Saunders WC, Bouwes N, Jordan C. Evaluating impacts using a BACI design, ratios, and a Bayesian approach with a focus on restoration. Environ Monit Assess. 2016; 188 (555) doi: 10.1007/s10661-016-5526-6

Dymond CC, Neilson ET, Stinson G, Porter K, MacLean DA, Gray DR, Campagna M, Kurz WA. Future spruce budworm outbreak may create a carbon source in eastern Canadian forests. Ecosystems. 2010; 13: 917–931. DOI: 10.1007/s10021-010-9364-z

Fargione J, Hill J, Tilman D, Polasky S, Hawthorne P. Land clearing and the biofuel carbon debt. Science (80-.). 2008; 319: 1235–1238. DOI: 10.1126/science.1152747

Fernández-Martínez M, Vicca S, Janssens IA, Sardans J, Luyssaert S, Campioli M, Chapin FS III, Ciais P, Malhi Y, Obersteiner M, Papale D, et al. Nutrient availability as the key regulator of global forest carbon balance. Nat Clim Change. 2014; 4: 471.

Fink AH, Brücher T, Ermert V, Krüger A, Pinto JG. The European storm Kyrill in January 2007: synoptic evolution, meteorological impacts and some considerations with respect to climate change. Nat Hazards Earth Syst Sci Discuss. 2009; 9: 405–423. DOI: 10.5194/nhess-9-405-2009

Fleischer P, Pichler V, Fleischer P Jr, Holko L, Máliš F, Gömöryová E, Cudlín P, Holeksa J, Homolová Z, Škvarenina J, St K, et al. Forest ecosystem services affected by natural disturbances, climate and land-use changes in the Tatra Mountains. Clim Chang Res Lett. 2017; 73: 57–71. DOI: 10.3354/cr01461

Foster DR, Knight DH, Franklin JF. Landscape patterns and legacies resulting from large, infrequent forest disturbances. Ecosystems. 1998; 1: 497–510. DOI: 10.1007/s100219900046

Friedlingstein P, Fung I, Holland EA, John J, Brasseur GP, Erickson D, Schimel D. On the contribution of CO2 fertilization to the missing biospheric sink. Glob Biogeochem Cycles. 1995; 19: 541–556. DOI: 10.1029/95GB02381

Friedlingstein P, Joel G, Field CB, Fung IY. Toward an allocation scheme for global terrestrial carbon models. Glob Chang Biol. 1999; 5: 755–770. DOI: 10.1046/j.1365-2486.1999.00269.x

Fu Z, Li D, Hararuk O, Schwalm C, Luo Y, Yan L. Recovery time and state change of terrestrial carbon cycle after disturbance. Environ Res Lett. 2017; 12 104004 doi: 10.1088/1748-9326/aa8a5c

Gibbs HK, Johnston M, Foley JA, Holloway T, Monfreda C, Ramankutty N, Zaks D. Carbon payback times for crop-based biofuel expansion in the tropics: the effects of changing yield and technology. Environ Res Lett. 2008; 3 doi: 10.1088/1748-9326/3/3/034001

Giorgi F, Jones C, Asrar GR. Addressing climate information needs at the regional level: the CORDEX framework. World Meteorol Organ Bull. 2009; 58: 175–183.

González-García M, Almeida AC, Hevia A, Majada J, Beadle C. Application of a process-based model for predicting the productivity of Eucalyptus nitens bioenergy plantations in Spain. Glob Change Biol Bioenergy. 2016; 8: 194–210. DOI: 10.1111/gcbb.12256

Goodale CL, Apps MJ, Birdsey RA, Field CB, Heath LS, Houghton RA, Jenkins JC, Kohlmaier GH, Kurz W, Liu S, Nabuurs GJ, et al. Forest carbon sinks in the Northern Hemisphere. Ecol Appl. 2002; 12: 891–899. DOI: 10.2307/3060997

Goulden ML, McMillan AMS, Winston GC, Rocha AV, Manies KL, Harden JW, Bond-Lamberty BP. Patterns of NPP, GPP, respiration, and NEP during boreal forest succession. Glob Change Biol. 2010; 17: 855–871. DOI: 10.1111/j.1365-2486.2010.02274.x

Grimm V, Revilla E, Berger U, Jeltsch F, Mooij WM, Railsback SF, Thulke H-H, Weiner J, Wiegand T, DeAngelis DL. Pattern-oriented modeling of agent-based complex systems: lessons from ecology. Science (80-.). 2005; 310: 987–991. DOI: 10.1126/science.111668

Gustafson EJ. When relationships estimated in the past cannot be used to predict the future: using mechanistic models to predict landscape ecological dynamics in a changing world. Landsc Ecol. 2013; 28: 1429–1437. DOI: 10.1007/s10980-013-9927-4

Halaj, J, Petráš, R. Rastové tabul ky hlavných drevín. Slovak Academic Press; Bratislava: 1998.

Hansen WD, Braziunas KH, Rammer W, Seidl R, Turner MG. It takes a few to tango: changing climate and fire regimes can cause regeneration failure of two subalpine conifers. Ecology. 2018; 99: 966–977. DOI: 10.1002/ecy.2181 [PubMed: 29464688]

Hanson PJ, Wullschleger SD, Norby RJ, Tschaplinski TJ, Gunderson CA. Importance of changing CO2, temperature, precipitation, and ozone on carbon and water cycles of an upland-oak forest: incorporating experimental results into model simulations. Glob Chang Biol. 2005; 11: 1402–1423. DOI: 10.1111/j.1365-2486.2005.00991.x

Harvey BJ, Donato DC, Turner MG. High and dry: post-fire tree seedling establishment in subalpine forests decreases with post-fire drought and large stand-replacing burn patches. Glob Ecol Biogeogr. 2016; 25: 655–669. DOI: 10.1111/geb.12443

Hlásny T, Barka I, Roessiger J, Kulla L, Trombik J, Sarvašová Z, Bucha T, Kovalcík M, Cihák T. Conversion of Norway spruce forests in the face of climate change: a case study in Central Europe. Eur J For Res. 2017; doi: 10.1007/s10342-017-1028-5

Hungerford, RD, Nemani, RR, Running, SW, Coughlan, JC. MTCLIM: A Mountain Microclimate Simulation Model. Odgen, UT: 1989.

Hyvönen R, Ågren GI, Linder S, Persson T, Cotrufo MF, Ekblad A, Freeman M, Grelle A, Janssens IA, Jarvis PG, Kellomäki S, et al. The likely impact of elevated [CO2], nitrogen deposition, increased temperature and management on carbon sequestration in temperate and boreal forest ecosystems: a literature review. New Phytol. 2007; 173: 463–480. DOI: 10.1111/j.1469-8137.2007.01967.x [PubMed: 17244042]

Janda P, Trotsiuk V, Mikoláš M, Bace R, Nagel TA, Seidl R, Seedre M, Morrissey RC, Kucbel S, Jaloviar P, Jasík M, et al. The historical disturbance regime of mountain Norway spruce forests in the Western Carpathians and its influence on current forest structure and composition. For Ecol Manage. 2017; 388: 67–78. DOI: 10.1016/j.foreco.2016.08.014 [PubMed: 28860676]

Johnstone JF, Allen CD, Franklin JF, Frelich LE, Harvey BJ, Higuera PE, Mack Michelle C, Meentemeyer RK, Metz MR, Perry GL, et al. Changing disturbance regimes, ecological memory, and forest resilience. Front Ecol Environ. 2016; 14: 369–378. DOI: 10.1002/fee.1311

Jones HP, Schmitz OJ. Rapid recovery of damaged ecosystems. PLoS One. 2009; 4 doi: 10.1371/journal.pone.0005653

Jonker JGG, Junginger M, Faaij A. Carbon payback period and carbon offset parity point of wood pellet production in the South-eastern United. Glob Change Biol Bioenergy. 2014; 6: 371–389. DOI: 10.1111/gcbb.12056

Kashian DM, Romme WH, Tinker DB, Turner MG, Ryan MG. Postfire changes in forest carbon storage over a 300-year chronosequence of Pinus contortadominated forests. Ecol Monogr. 2013; 83: 49–66. DOI: 10.1890/11-1454.1

Keane, RE, Loehman, RA, Holsinger, LM. Gen Tech Rep. Fort Collins, CO; U.S.: 2011. The FireBGCv2 landscape fire and succession model: a research simulation platform for exploring fire and vegetation dynamics. RMRS-GTR-255

Keenan TF, Gray J, Friedl MA, Toomey M, Bohrer G, Hollinger DY, Munger JW, O'Keefe J, Schmid HP, Wing IS, Yang B, et al. Net carbon uptake has increased through warming-induced changes in temperate forest phenology. Nat Clim Change. 2014; 4: 598–604. DOI: 10.1038/nclimate2253

Kulakowski D, Seidl R, Holeksa J, Kuuluvainen T, Nagel TA, Panayotov M, Svoboda M, Thorn S, Vacchiano G, Whitlock C, Wohlgemuth T, et al. Forest ecology and management a walk on the wild sid: disturbance dynamics and the conservation and management of European mountain forest ecosystems. For Ecol Manag. 2017; 388: 120–131. DOI: 10.1016/j.foreco.2016.07.037

Kunca A, Zúbrik M, Galko J, Vakula J, Leontovyč R, Konôpka B, Nikolov C, Gubka A, Longauerová V, Malová M, Kaštier P, et al. Salvage felling in the Slovak forests in the period 2004-2013. For J. 2015; 61: 188–195. DOI: 10.1515/forj-2015-0027

Kurz WA, Dymond CC, Stinson G, Rampley GJ, Neilson ET, Carroll AL, Ebada T, Safranyik L. Mountain pine beetle and forest carbon feedback to climate change. Nature. 2008a; 452: 987–990. DOI: 10.1038/nature06777 [PubMed: 18432244]

Kurz WA, Stinson G, Rampley G. Could increased boreal forest ecosystem productivity offset carbon losses from increased disturbances? Philos Trans Biol Sci. 2008b; doi: 10.1098/rstb.2007.2198

Lamers P, Junginger M. The "debt" is in the detail: a synthesis of recent temporal forest carbon analyses on woody biomass forenergy. Biofuels Bioprod Biorefining. 2013; 7: 373–385. DOI: 10.1002/bbb.1407

Lamers P, Junginger M, Dymond CC, Faaij A. Damaged forests provide an opportunity to mitigate climate change. Gcb Bioenergy. 2014; 6: 44–60. DOI: 10.1111/gcbb.12055

Landsberg JJ, Waring RH. A generalised model of forest productivity using simplified concepts of radiation-use efficiency, carbon balance and partitioning. For Ecol Manag. 1997; 95: 209–228. DOI: 10.1016/S0378-1127(97)00026-1

Lindner M, Fitzgerald JB, Zilmmermann NE, Reyer C, Delzon S, van der Maaten E, Schelhaas M-J, Lasch P, Eggers J, van der Maaten-Theunissen M, Suckow F, et al. Climate change and European forests: what do we know, what are the uncertainties, and what are the implications for forest management? J Environ Manan. 2014; 146: 69–83. DOI: 10.1016/j.jenvman.2014.07.030

Lindroth A, Lagergren F, Grelle A, Klemedtsson L, Langvall O, Weslien P, Tuulik J. Storms can cause Europe-wide reduction in forest carbon sink. Glob Change Biol. 2009; 15: 346–355. DOI: 10.1111/j.1365-2486.2008.01719.x

Liu S, Bond-Lamberty B, Hicke JA, Vargas R, Zhao S, Chen J, Edburg SL, Hu Y, Liu J, McGuire AD, Xiao J, et al. Simulating the impacts of disturbances on forest carbon cycling in North America: processes, data, models, and challenges. J Geophys Res Biogeosci. 2011a; 116: 1–22. DOI: 10.1029/2010JG001585

Liu S, Bond-Lamberty B, Hicke JA, Vargas R, Zhao S, Chen J, Edburg SL, Hu Y, Liu J, McGuire AD, Xiao J, et al. Simulating the impacts of disturbances on forest carbon cycling in North America: processes, data, models, and challenges. J Geophys Res Biogeosci. 2011b; 116 G00K08 doi: 10.1029/2010JG001585

Lloret F, Keeling EG, Sala A. Components of tree resilience: effects of successive low-growth episodes in old ponderosa pine forests. Oikos. 2011; 120: 1909–1920. DOI: 10.1111/j.1600-0706.2011.19372.x

Luyssaert S, Inglima I, Jung M, Richardson AD, Reichstein M, Papape D, Piao SL, Schulze E-D, Wingate L, Matteucci G, Aragao L, et al. CO2 balance of boreal, temperate, and tropical forests derived from a global database. Glob Change Biol. 2007; 13: 2509–2537. DOI: 10.1111/j.1365-2486.2007.01439.x

Mäkelä A. Process-based modelling of tree and stand growth: towards a hierarchical treatment of multiscale processes. Can J For Res. 2003; 33: 398–409. DOI: 10.1139/x02-130

Mayer M, Sandén H, Rewald B, Godbold DL, Katzensteiner K. Increase in heterotrophic soil respiration by temperature drives decline in soil organic carbon stocks after forest windthrow in a mountainous ecosystem. Funct Ecol. 2017; 31: 1163–1172. DOI: 10.1111/1365-2435.12805

Medlyn BE, Barton CVM, Broadmeadow MSJ, Ceulemans R, De Angelis P, Forstreuter M, Freeman M, Jackson SB, Kellomäki S, Laitat E, Rey A, et al. Stomatal conductance of forest species after long-term exposure to elevated CO2 concentration: a synthesis. New Phytol. 2001; 149: 247–264. DOI: 10.1046/j.1469-8137.2001.00028.x [PubMed: 33874628]

Metsaranta JM, Dymond CC, Kurz WA, Spittlehouse DL. Uncertainty of 21st century growing stocks and GHG balance of forests in British Columbia, canada resulting from potential climate change impacts on ecosystem processes. For Ecol Manag. 2011; 262: 827–837. DOI: 10.1016/j.foreco.2011.05.016

Mina M, Martin-Benito D, Bugmann H, Cailleret M. Forward modeling of tree-ring width improves simulation of forest growth responses to drought. Agric For Meteorol. 2016; 221: 13–33. DOI: 10.1016/j.agrformet.2016.02.005

Minunno F, Xenakis G, Perks MP, Mencuccini M. Calibration and validation of a simplified process-based model for the prediction of the carbon balance of Scottish Sitka spruce (Picea sitchensis) plantations. Can J For Res. 2010; 40: 2411–2426. DOI: 10.1139/X10-181

Moore DJP, Trahan NA, Wilkes P, Quaife T, Stephens BB, Elder K, Desai AR, Negron J, Monson RK. Persistent reduced ecosystem respiration after insect disturbance in high elevation forests. Ecol Lett. 2013; 16: 731–737. DOI: 10.1111/ele.12097 [PubMed: 23496289]

Moss RH, Edmonds JA, Hibbard KA, Manning MR, Rose SK, van Vuuren DP, Carter TR, Emori S, Kainuma M, Kram T, Meehl GA, et al. The next generation of scenarios for climate change research and assessment. Nature. 2010; 463: 747–756. DOI: 10.1038/nature08823 [PubMed: 20148028]

Murray FW. On the computation of saturation vapor pressure. J Appl Meteorol Climatol. 1967; 6: 203–204. DOI: 10.1175/1520-0450(1967)006<0203:OTCOSV>2.0.CO;2

Pan Y, Birdsey RA, Fang J, Houghton R, Kauppi PE, Kurz WA, Phillips OL, Shvidenko A, Lewis SL, Canadell JG, Ciais P, et al. A large and persistent carbon sink in the world's forests. Science (80-.). 2011; 333: 988–993. DOI: 10.1126/science.1201609

Peters EB, Wythers RK, Bradford JB, Reich PB. Influence of disturbance on temperate forest productivity. Ecosystems. 2013; 16: 95–110. DOI: 10.1007/s10021-012-9599-y

R Core Team. R: a Language and Environment for Statistical Computing. 2016.

Rammer W, Seidl R. Coupling human and natural systems: simulating adaptive management agents in dynamically changing forest landscapes. Glob Environ Change. 2015; 35: 475–485. DOI: 10.1016/j.gloenvcha.2015.10.003

Reineke LH. Perfecting a stand-density index for even-aged forests. J Agric Res. 1933; 46: 627–638.

Reyer C, Lasch-Born P, Suckow F, Gutsch M, Murawski A, Pilz T. Projections of regional changes in forest net primary productivity for different tree species in Europe driven by climate change and carbon dioxide. Ann For Sci. 2014; 71: 211–225. DOI: 10.1007/s13595-013-0306-8

Rizman I, et al. Knowledge-base on species composition in site units of forest typology for average (typical) conditions of Slovakia. Natl For Centre Electron Mater. 2005.

Seidl R, Rammer W. Climate change amplifies the interactions between wind and bark beetle disturbances in forest landscapes. Landsc Ecol. 2017; 32: 1485–1498. DOI: 10.1007/s10980-016-0396-4 [PubMed: 28684889]

Seidl R, Rammer W, Scheller RM, Spies TA. An individual-based process model to simulate landscape-scale forest ecosystem dynamics. Ecol Modell. 2012a; 231: 87–100. DOI: 10.1016/j.ecolmodel.2012.02.015

Seidl R, Spies TA, Rammer W, Steel EA, Pabst RJ, Olsen K. Multi-scale drivers of spatial variation in old-growth forest carbon density disentangled with lidar and an individual-based landscape model. Ecosystems. 2012b; 15: 1321–1335. DOI: 10.1007/s10021-012-9587-2

Seidl R, Rammer W, Spies TA. Disturbance legacies increase the resilience of forest ecosystem structure, composition, and functioning. Ecol Appl. 2014a; 24: 2063–2077. DOI: 10.1890/14-0255.1 [PubMed: 27053913]

Seidl R, Schelhaas M-J, Rammer W, Verkerk PJ. Increasing forest disturbances in Europe and their impact on carbon storage. Nat Clim Change. 2014b; 4: 806–810. DOI: 10.1038/nclimate2318

Seidl R, Spies TA, Peterson DL, Stephens SL, Jeffrey A. Searching for resilience: addressing the impacts of changing disturbance regimes on forest ecosystem services. J Appl Ecol. 2016; 53: 120–129. DOI: 10.1111/1365-2664.12511 [PubMed: 26966320]

Seidl R, Thom D, Kautz M, Martin-Benito D, Peltoniemi M, Vacchiano G, Wild J, Ascoli D, Petr M, Honkaniemi J, Lexer MJ, et al. Forest disturbances under climate change. Nat Clim Change. 2017a; 7: 395–402. DOI: 10.1038/nclimate3303

Seidl R, Vigl F, Rössler G, Neumann M, Rammer W. Assessing the resilience of Norway spruce forests through a model-based reanalysis of thinning trials. For Ecol Manag. 2017b; 388: 3–12. DOI: 10.1016/j.foreco.2016.11.030

Seidl R, Albrich F, Thom D, Rammer W. Harnessing landscape heterogeneity for managing future disturbance risks in forest ecosystems. J Environ Manang. 2018; 209: 46–56. DOI: 10.1016/j.jenvman.2017.12.014

Senf C, Pflugmacher D, Hostert P, Seidl R. Using Landsat time series for characterizing forest disturbance dynamics in the coupled human and natural systems of Central Europe. ISPRS J Photogramm Remote Sens. 2017; 130: 453–463. DOI: 10.1016/j.isprsjprs.2017.07.004 [PubMed: 28860678]

Silva Pedro M, Rammer W, Seidl R. Tree species diversity mitigates disturbance impacts on the forest carbon cycle. Oecologia. 2015; 177: 619–630. DOI: 10.1007/s00442-014-3150-0 [PubMed: 25526843]

Smith NG, Dukes JS. Plant respiration and photosynthesis in global-scale models: incorporating acclimation to temperature and CO2. Glob Change Biol. 2012; 19: 45–63. DOI: 10.1111/j.1365-2486.2012.02797.x

Solberg S, Dobbertin M, Reinds GJ, Lange H, Andreassen K, Garcia F, Hildingsson A, de Vries W. Analyses of the impact of changes in atmospheric deposition and climate on forest growth in European monitoring plots: a stand growth approach. For Ecol Manag. 2009; 258: 1735–1750. DOI: 10.1016/j.foreco.2008.09.057

Spiecker, H, Hansen, J, Klimo, E, Skovsgaard, JP, Sterba, H, von Teuffel, K. Norway Spruce Conversion – Options and Consequences. Brill; Leiden: 2004.

Stadelmann G, Bugmann H, Meier F, Wermelinger B, Bigler C. Effects of salvage logging and sanitation felling on bark beetle (Ips typographus L.) infestations. For Ecol Manag. 2013; 305: 273–281. DOI: 10.1016/j.foreco.2013.06.003

Štepánek P, Zahradnícek P, Farda A, Skalák P, Trnka M, Meitner J, Rajdl K. Projection of drought-inducing climate conditions in the Czech Republic according to Euro-CORDEX models. Clim Chang Res Lett. 2016; 70: 179–193. DOI: 10.3354/cr01424

Strandberg G, Bärring L, Hansson U, Jansson C, Jones C, Kjellström E, Kolax M, Kupiainen M, Nikulin G, Samuelsson P, Ullerstig A, et al. CORDEX scenarios for Europe from the Ross by Centre regional climate model RCA4. SMHI Rep Meteorol Climatol. 2014; 116: 1–45.

Thom D, Seidl R, Steyrer G, Krehan H, Formayer H. Slow and fast drivers of the natural disturbance regime in Central European forest ecosystems. For Ecol Manag. 2013; 307: 293–302. DOI: 10.1016/j.foreco.2013.07.017

Thom D, Rammer W, Dirnböck T, Müller J, Kobler J, Katzensteiner K, Helm N, Seidl R. The impacts of climate change and disturbance on spatio-temporal trajectories of biodiversity in a temperate forest landscape. J Appl Ecol. 2017a; 54: 28–38. DOI: 10.1111/1365-2664.12644 [PubMed: 28111479]

Thom D, Seidl R, Rammer W. The impact of future forest dynamics on climate: interactive effects of changing vegetation and disturbance regimes. Ecol Monogr. 2017b; 87: 665–684. DOI: 10.1002/ecm.1272 [PubMed: 29628526]

Thomas FM, Bögelein R, Werner W. Interaction between Douglas fir and European beech -Investigations in pure and mixed stands. Forstarchiv. 2015; 86: 83–91. DOI: 10.4432/0300-4112-86-83

Thuille A, Buchmann N, Schulze ED. Carbon stocks and soil respiration rates during deforestation, grassland use and subsequent Norway spruce afforestation in the Southern Alps, Italy. Tree Physiol. 2000; 20: 849–857. DOI: 10.1093/treephys/20.13.849 [PubMed: 11303575]

Turner MG. Disturbance and landscape dynamics in a changing world. Ecology. 2010; 91: 2833–2849. DOI: 10.1890/10-0097.1 [PubMed: 21058545]

van Meijgaard, E, van Ulft, LH, van de Berg, WJ, Bosveld, FC, van den Hurk, B, Lenderink, G, Siebesma, AP. Technical Report 302: the KNMI Regional Atmospheric Climate Model RACMO Version 2.1. De Bilt: 2008.

van Oijen M, Reyer C, Bohn FJ, Cameron DR, Deckmyn G, Flechsig M, Härkönen S, Hartig F, Huth A, Kiviste A, Lasch P, et al. Bayesian calibration, comparison and averaging of six forest models, using data from Scots pine stands across Europe. For Ecol Manage. 2013; 289: 255–268. DOI: 10.1016/j.foreco.2012.09.043

Wang W, Xiao J, Ollinger SV, Desai AR, Chen J, Noormets A. Quantifying the effects of harvesting on carbon fluxes and stocks in northern temperate forests. Biogeosciences. 2014; 11: 6667–6682. DOI: 10.5194/bg-11-6667-2014

White JW, Rassweiler A, Samhouri JF, Stier AC, White C. Ecologists should not use statistical significance tests to interpret simulation model results. Oikos. 2014; 123: 385–388. DOI: 10.1111/j.1600-0706.2013.01073.x

Williams CA, Collatz GJ, Masek J, Goward SN. Carbon consequences of forest disturbance and recovery across the conterminous United States. Glob Biogeochem Cycles. 2012; 26: 1–13. DOI: 10.1029/2010GB003947

Williams AP, Allen CD, Macalady AK, Griffin D, Woodhouse CA, Meko DM, Swetnam TW, Rauscher SA, Seager R, Grissino-Mayer HD, Dean JS, et al. Temperature as a potent driver of regional forest drought stress and tree mortality. Nat Clim Change. 2013; 3: 292–297. DOI: 10.1038/nclimate1693

Yoda K, Kira T, Ogawa H, Hozumi K. elf-thinning in overcrowded pure stands under cultivated and natural condition. J Inst Polytech Osaka City Univ Ser D, Biol. 1963; 14: 107–129.

Yue C, Ciais P, Zhu D, Wang T, Peng SS, Piao SL. How have past fire disturbances contributed to the current carbon balance of boreal ecosystems? Biogeosciences. 2016; 13: 675–690. DOI: 10.5194/bg-13-675-2016

Zehetgruber B, Kobler J, Dirnböck T, Jandl R, Seidl R, Schindlbacher A. Intensive ground vegetation growth mitigates the carbon loss after forest disturbance. Plant Soil. 2017; 1–14. DOI: 10.1007/s11104-017-3384-9

Zeng N, Qian H, Roedenbeck C, Heimann M. Impact of 1998-2002 midlatitude drought and warming on terrestrial ecosystem and the global carbon cycle. Geophys Res Lett. 2005; 32 L22709 doi: 10.1029/2005GL024607

Zhao M, Running SW. Drought-induced reduction in global terrestrial net primary production from 2000 through 2009. Science (80-.). 2010; (329) 940–943. DOI: 10.1126/science.1192666

Zhou T, Shi P, Jia G, Dai Y, Zhao X, Shangguan W, Du L, Wu H, Luo Y. Age-dependent forest carbon sink: estimation via inverse modeling. J Geophys Res Biogeosciences. 2015; 120: 2473–2492. DOI: 10.1002/2015JG002943

Zhu Q, Zhuang Q. Influences of calibration data length and data period on model parameterization and quantification of terrestrial ecosystem carbon dynamics. Geosci Model Dev Discuss. 2013; 6: 6835–6865. DOI: 10.5194/gmdd-6-6835-2013

Europe PMC Funders Author Manuscripts

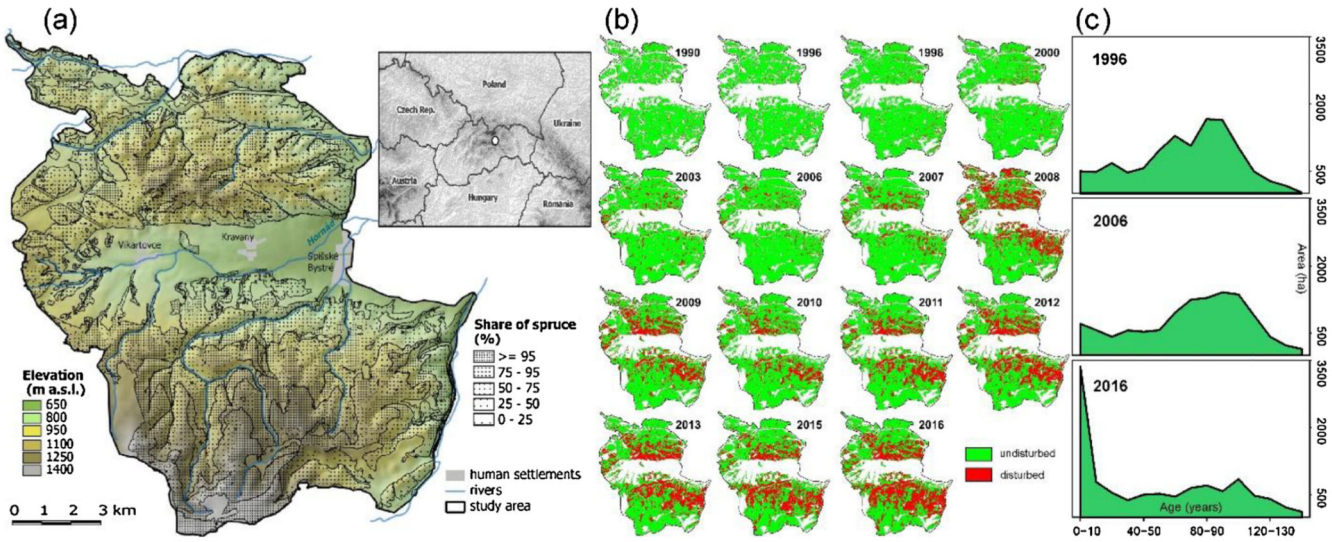

Fig. 1.

Map of the study region and its location in Central Europe. Forest area, share of Norway spruce and elevation are indicated (a). Time series of classified Landsat satellite imagery indicating the progression and extent of forest disturbance in the period 1990–2016 (b). Development of forest age structure derived from forest management plans during the disturbance episode (c).

Europe PMC Funders Author Manuscripts

Europe PMC Funders Author Manuscripts

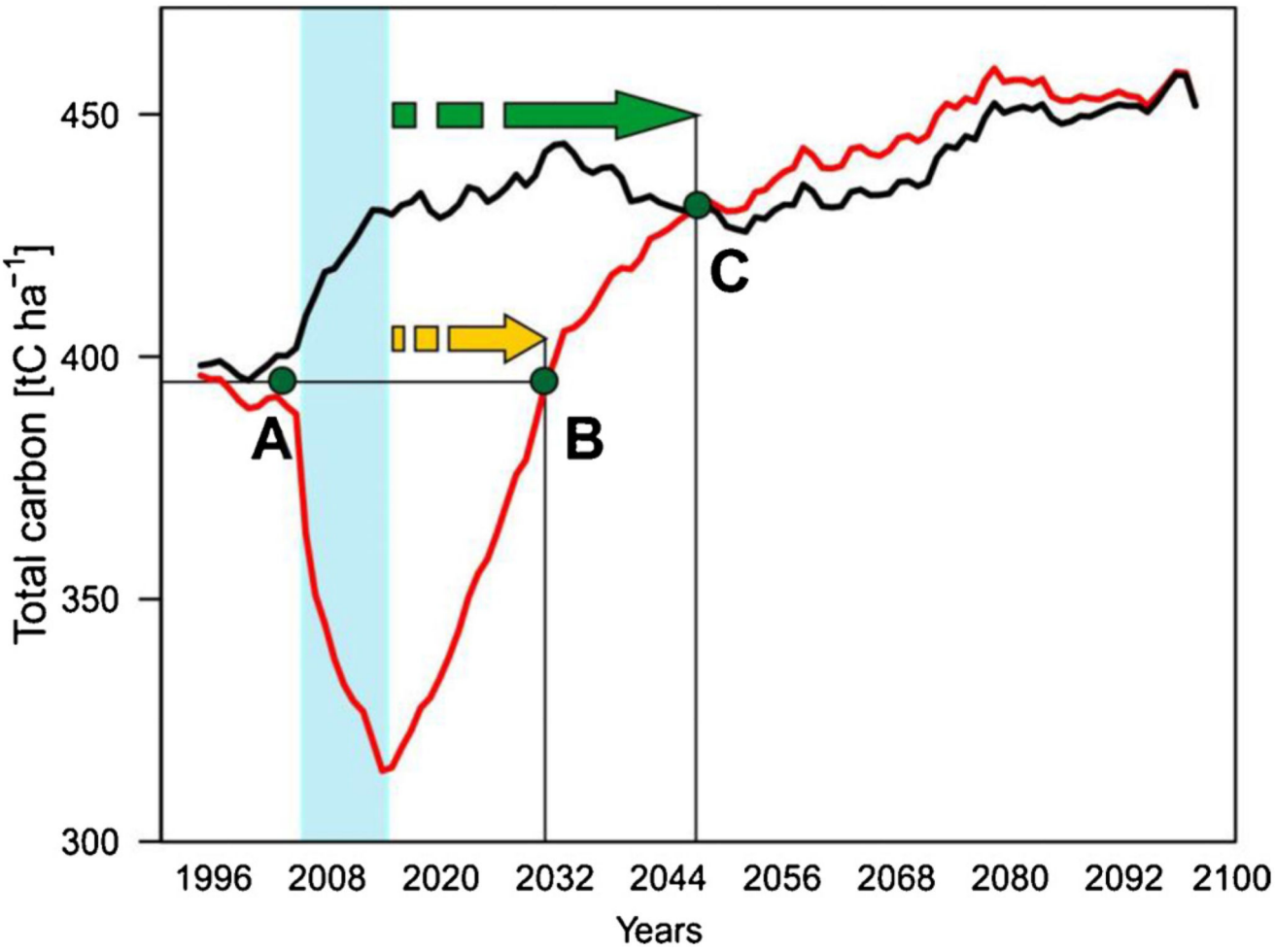

Fig. 2.

Scheme for the assessment of C recovery after disturbance. Red line – simulated disturbed development; black line – simulated undisturbed development; blue rectangle – disturbance episode; yellow arrow – time from the end of disturbance episode to the year when the pre-disturbance C_{total} is recovered (payback); green arrow – time from the end of disturbance event to the year when the undisturbed development is reached (parity); A – pre-disturbance C_{total}; B – year of C payback time; C – year of C parity (For interpretation of the references to colour in this figure legend, the reader is referred to the web version of this article.).

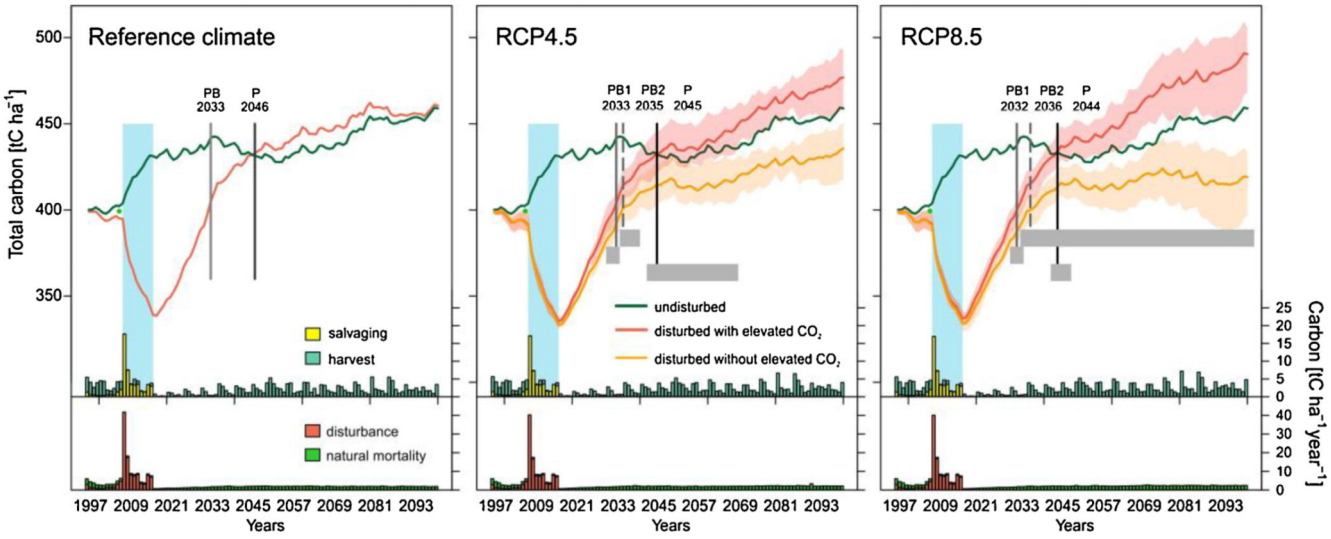

Fig. 3.

Simulated total ecosystem carbon (C_{total}) and its post-disturbance recovery. The disturbed forest development is simulated under three different climate conditions, as well as with and without the fertilizing effect of CO_2. The reference undisturbed development was generated under reference climate corresponding to the period 1961-1990. Simulations under climate change are driven by seven climate models for each RCP scenario; solid lines indicate the average projection and shaded envelopes indicate the minimum–maximum range of the simulations. Grey rectangles indicate the inter-model range of payback time (PB1 with elevated CO_2; PB2 without elevated CO_2) and the C parity (P). Columns at the bottom indicate the annual C amount removed from the landscape by harvests and salvage cutting, and the annual C in dead trees. In case of RCP scenarios, columns show multi-model means under elevated CO_2 level. The blue vertical rectangle indicates the wind-bark beetle disturbance episode investigated here (For interpretation of the references to colour in this figure legend, the reader is referred to the web version of this article.).

Europe PMC Funders Author Manuscripts

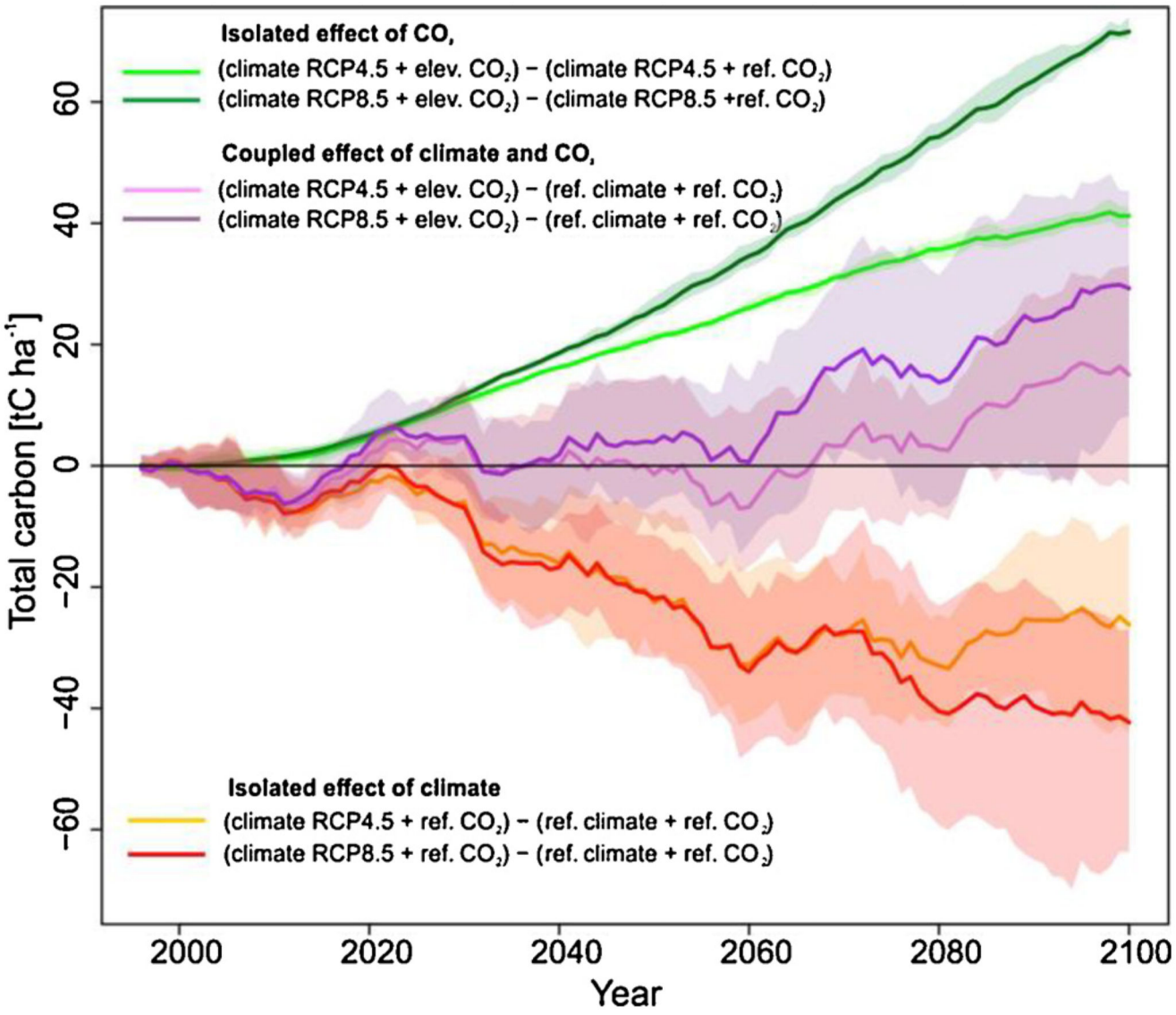

Fig. 4.

Isolated and coupled effects of changing climate and elevated CO_2 concentrations on the disturbed development of the total ecosystem carbon (C_{total}). Each line shows difference between two simulations, based on the equations indicated in the figure.

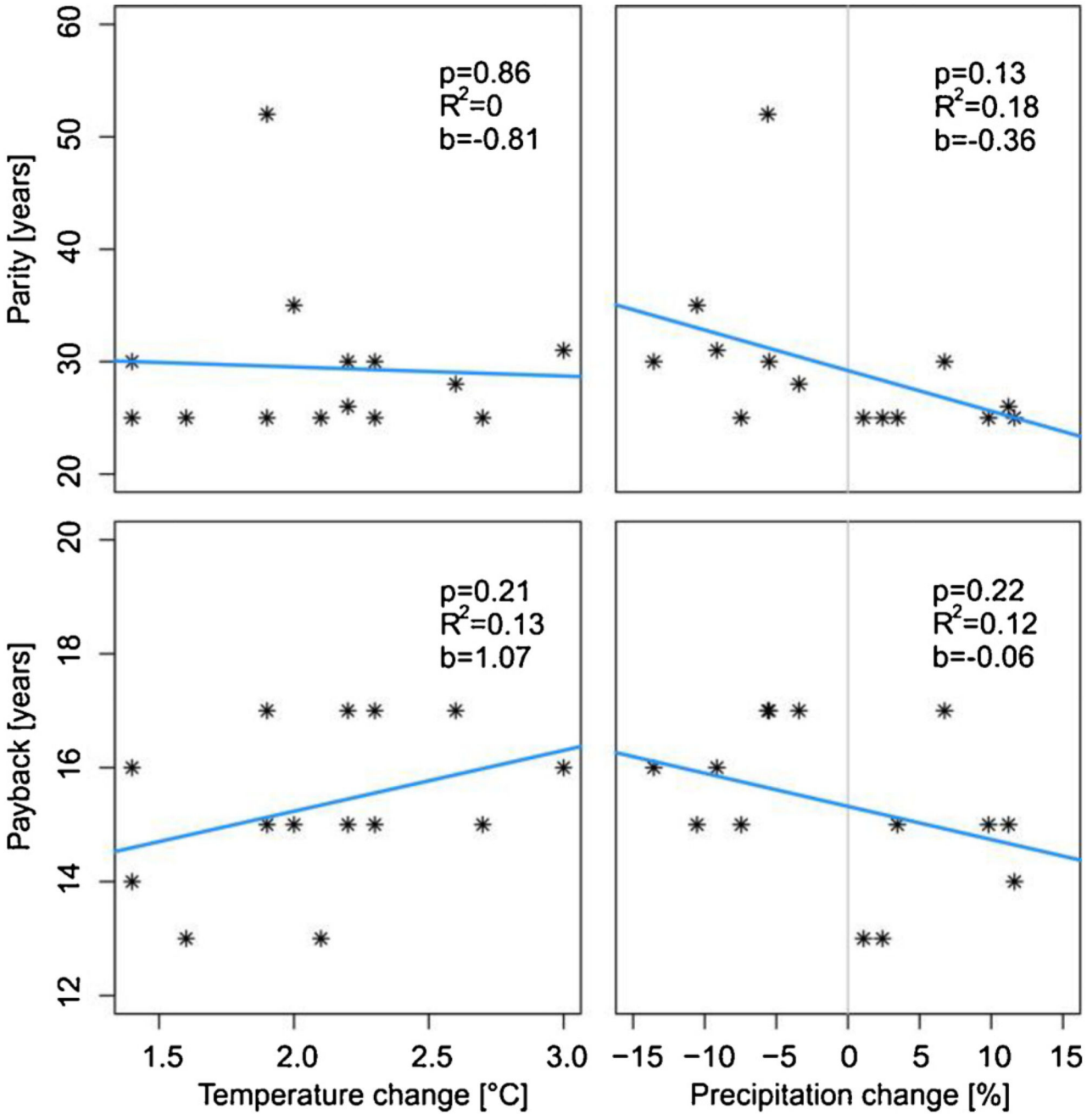

Fig. 5.

Response of C cycle recovery indicators to projected changes in air temperature and precipitation during the growing season (IV-IX), derived from seven climate models driven by two RCP scenarios (see also Appendix A).

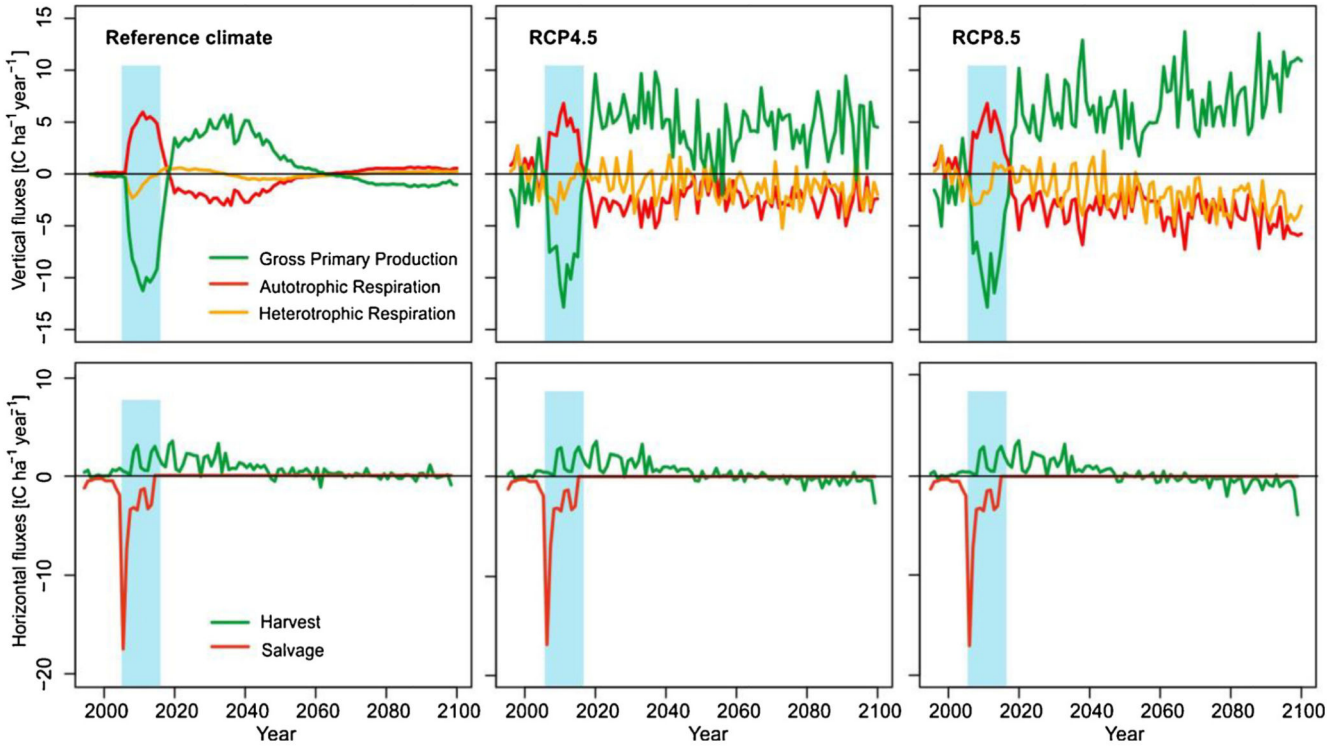

Fig. 6.

Main horizontal and vertical carbon fluxes during the simulation period. Blue rectangle indicates the disturbance episode 2008–2016. The lines show the difference of disturbed trajectories to undisturbed forest development under three climates. In the panels for RCP scenarios, the difference is calculated as (disturbed development under climate change) – (undisturbed development under reference climate); thus the graphs present the combined effect of disturbance and climate change (For interpretation of the references to colour in this figure legend, the reader is referred to the web version of this article.).

Europe PMC Funders Author Manuscripts

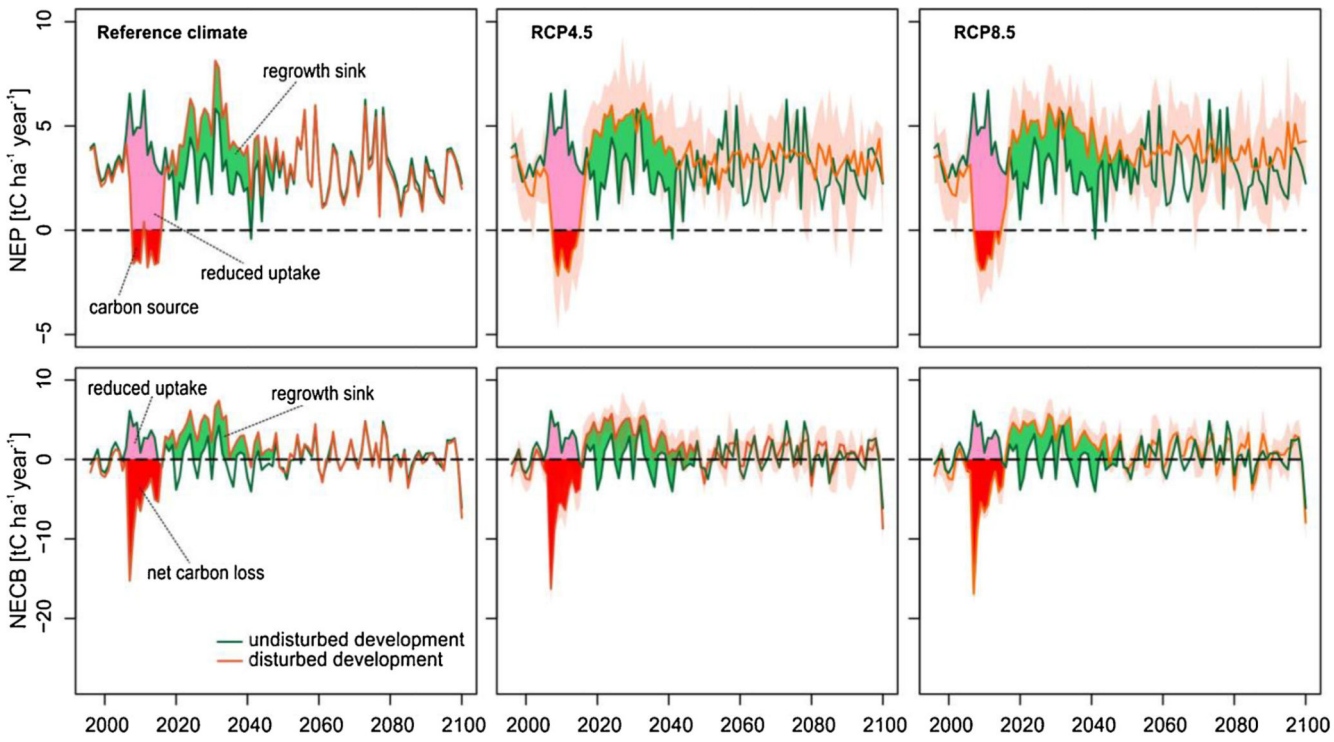

Fig. 7.

Disturbed and undisturbed development of Net Ecosystem Production (NEP, first row) and Net Ecosystem Carbon Balance (NECB, second row). The undisturbed development is simulated under reference climate in all cases. Future climate projections under the RCP4.5 and 8.5 scenarios are based on seven GCM-RCM combinations; solid lines indicate the multi-model means and envelopes indicate the minimum–maximum range of the seven projections. The pink and red areas indicate the reduced uptake and net C release due to the disturbance, respectively. The green area indicates the increased C uptake after disturbance (legacy sink effect) (For interpretation of the references to colour in this figure legend, the reader is referred to the web version of this article.).

Europe PMC Funders Author Manuscripts

Table 1

Reference climate and projected changes in major climate variables driving forest development. The values indicate spatial averages across the landscape for 30-year time periods. Temperatures are the annual averages of daily minimum and maximum values. In case of climate model predictions, means and standard deviations are calculated based on seven GCM-RCM combinations (see also Appendix A).

	Observed[a]	Model past[b]	RCP4.5[b]		RCP8.5[b]	
	1971–2000	1971–2000	2021–2050	2071–2100	2021–2050	2071–2100
Minimum temperature [°C]	0.2	0.2 ± 0.03	1.7 ± 0.4	2.8 ± 0.6	1.9 ± 0.4	4.9 ± 0.7
Maximum temperature [°C]	9.7	9.9 ± 0.04	11.3 ± 0.4	12.5 ± 0.6	11.5 ± 0.5	14.7 ± 0.8
Growing season precipitation [mm]	598	576 ± 16	580 ± 19	592 ± 67	608 ± 20	577 ± 72
Vapour pressure deficit [kPa]	0.32	0.32 ± 0.00	0.35 ± 0.01	0.38 ± 0.02	0.35 ± 0.01	0.45 ± 0.04

[a] data from weather station recalculated over the study area by MTClim.

[b] climate model results recalculated to the position of weather station and then over the study landscape by MTClim.

Table 2

Evaluation of simulated productivity against data from Forest Management Plans and National Forest Inventory.

Tree species / Statistics	N	Share (%)[a]	R-square	Mean SI[b] [observed]	Mean SI [simulated]	Bias	StDev of SI [observed]	StDev of SI [simulated]	Difference of StDevs	5–95 %[c] of SI [observed]	5–95 %[c] of SI [simulated]	
Reference data: Forest Management Plans												
Picea abies	130	100	0.52	28.52	29.83	1.31	3.24	1.92	–1.32	22.9–34.0	26.4–32.6	
Fagus sylvatica	80	45–100	0.89	24.98	24.76	–0.22	3.64	2.31	–1.33	18.0–30.0	21.2–28.1	
Abies alba	116	41–100	0.74	24.28	25.12	0.84	2.92	2.00	–0.92	20.0-28.0	22.0–28.4	
Pinus sylvestris	109	74–100	0.31	20.88	19.41	–1.47	3.37	1.68	–1.70	16.0–28.0	16.8–22.5	
Larix decidua	96	67–100	0.87	24.73	22.65	–2.08	4.00	2.00	–2.00	20.0–30.0	20.2–25.9	
Average[d]	–	–	0.67	24.68	24.35	–0.32	3.43	1.98	–1.45	–	–	
Weighted average[e]	–	–	0.55	27.24	27.91	0.67	3.33	1.92	–	1.41	–	–
Reference data: National Forest Inventory												
Picea abies	30	48–100		27.6	33.21	5.61	5.67	2.73	–2.94	22–40	27.8–36.4	
Fagus sylvatica	8	13–37	0.71	25.25	21.75	–3.5	6.5	4	–2.5	18.7–35.3	16.3–26.4	
Abies alba	4	9–16	0.94	25.5	17.98	–7.51	7.55	5.27	–2.28	18.9–34.2	13–24	
Pinus sylvestris	4	17–25	0.07	22	18.74	–3.26	2.83	1.61	–1.22	18.6–24	16.8–19.9	
Larix decidua	No data											
Average[d]	–	–	0.47	25.88	22.92	–2.17	5.64	3.40	–2.24	–	–	
Weighted average>[e]	–	–	0.19	26.71	30.98	4.07	5.46	2.73	–2.73	–	–	

[a] Share of the species in a stand (%).

[b] SI – Site Index, i.e. mean stand height at age 100 in meters.

[c] 5th and 95th percentiles.

[d] Arithmetic mean over all species.